Chapter

Fiber Composites Made of Low-Dimensional Carbon Materials

Yan Xu and Xian Zhang

Abstract

In recent years, a scientific shift has been observed that the use of carbon-based nanomaterials in different composite materials can improve their mechanical, thermal, and electrical properties. Different carbon-based nanomaterials have various structures and mechanical, electrical, and thermal conductivity characteristics. By combining with different material composite methods, carbon composite materials with different structures can be prepared. Through the optimization of material structure, carbon composite materials with high performance can be obtained. SP^2 hybrid carbon materials, such as carbon nanotubes (CNTs), carbon fiber (CF), and graphene, have excellent electrical, thermal, and mechanical properties due to their regular carbon six-membered ring structure, so they are the main low-dimensional carbon materials and are widely used in composite research. In this chapter, the research progress of carbon nanotubes, carbon fibers, and graphene-based fibers (GBFs) in composite materials are introduced, respectively, and the preparation method, molding process, performance, and application in industry are summarized. Finally, the existing problems and future development trend of carbon-based composites are prospected.

Keywords: carbon-based nanomaterials, carbon nanotubes (CNTs), carbon fibers (CF), graphene-based fibers (GBFs), fiber composites

1. Introduction

Among all kinds of low-dimensional materials [1–8], using carbon-based low-dimensional materials to improve their physical, mechanical, and electrical properties has become a trend [9]. These carbon-based nano/micron additives include carbon fibers (CF), single-walled and multi-walled carbon nanotubes (SWCNTs and MWCNTs) [10–12], graphene oxide (GO) [13–15], and graphene nanoplates (GNP) [16]. The results show that the composites with high strength ductility, dimensional stability, and economy can be produced. They have an attractive application prospect in the fields of microelectronic devices, aerospace, energy, chemical industry, etc.

Different carbon material units have various structures and mechanical, thermal, and electrical properties. By combining with different material composite methods, carbon composite materials with different structures can be prepared. Through the optimization of material structure, carbon composite materials with high performance can be obtained [17, 18]. This chapter mainly introduces the preparation methods, properties, and application fields of carbon-based nanomaterials, such as CNTs,

CF, and GBFs, which are commonly used to assemble macro carbon composites. The preparation methods of GBFs and their composite fibers, as well as their applications in sensors, energy storage, energy conversion, and other aspects, such as supercapacitors, lithium-ion batteries (LIBs), actuators, and solar cells, are mainly introduced. Finally, the existing problems and future development of carbon-matrix composites are summarized.

2. Carbon nanotubes (CNTs)

CNTs were first discovered under TEM in 1991. It is a one-dimensional tubular material made of SP^2 hybrid carbon atoms. Its diameter ranges from several nanometers to tens of nanometers, and its length can reach centimeter-level at most. According to the wall layer, it can be divided into single-walled CNTs (SWCNTs) and multi-walled CNTs (MWCNTs) (**Figure 1**). It is the most commercialized nanofiber with the highest strength and the smallest diameter [19–21]. Moreover, CNTs have good toughness, which can withstand 40% of tensile strain without brittle behavior or fracture phenomenon, thus improving the toughness of matrix composite [22]. CNTs with super high aspect ratio and excellent mechanical and physical properties, such as high strength, high thermal conductivity, high conductivity, and low thermal expansion coefficient, are regarded as the ideal functional modifier for preparing high-performance composite materials [23–25].

2.1 Fabrication of CNTs

The preparation methods of CNTs include chemical vapor deposition (CVD), arc discharge (AD), and laser ablation (LA) [26]. CVD is the most commonly used method to prepare CNTs in the laboratory. Generally, CNTs are grown under the action of the catalyst after carbon source cracking at a certain temperature. This method has a series of advantages, such as simple equipment, fast preparation speed, large output, and controllable quality. The catalysts are generally transition metals such as iron, cobalt, and nickel, and the carbon sources are generally carbon-containing organics such as methane, ethylene, acetylene, ethanol, and xylene. The morphology (diameter, wall layer, length, density, curvature, crystallinity, etc.) of CNTs can be tuned by controlling the type and concentration of catalyst, the ratio of carbon source and injection speed, the temperature, pressure, and time of CVD [27–30].

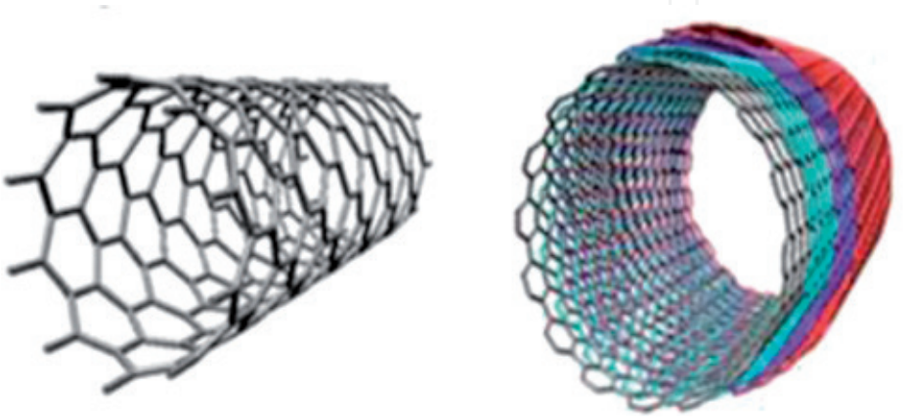

Figure 1.
Schematic diagrams of fullerene single-walled carbon nanotube (SWCNT) and multi-walled carbon nanotube (MWCNT) [19].

The AD method is also the main method to produce CNTs. Usually, in the low-pressure arc chamber of inert gas, hydrogen, or other gases, the graphite material is used as the electrode to generate a continuous arc between the electrodes, which makes the graphite react with the catalyst to generate CNTs. The AD method has a high yield, and the CNT's crystal structure is relatively complete [31, 32].

Laser ablation is a method to prepare CNTs by bombarding the surface of graphite target doped with iron, cobalt, nickel, and other transition metals in an inert gas environment at 1200°C [33]. The advantage of this method is that the CNTs produced are of high purity and convenient for continuous production, but this method is not suitable for large-scale macro production due to its high energy consumption, complex equipment, and high preparation cost [34, 35]. In addition to the above three main preparation methods, CNTs can also be prepared by template method, flame method, solar energy method, and electrolytic alkali metal halide method [36].

2.2 Properties of CNTs

Because of its special tubular structure and the strong binding force between SP^2 hybrid carbon atoms, CNTs have high strength, fracture toughness, and elastic modulus, which are superior to any one-dimensional fiber [37]. The tensile strength of CNTs can reach 50–800 GPa, nearly 100 times of that standard steel, about 200 times higher than that of other polymer fibers, and its structure can be kept intact under 1 million atmospheric pressure. CNTs will not break obviously under large bending, while graphite fiber will break when bending 1% (volume fraction). The maximum elastic modulus of CNTs is 1 TPa, which is equivalent to that of diamond and about five times to that of steel. Due to defects, the actual elastic modulus of MWCNTs is in the range of 20–50 GPa [38–40]. Fiber is usually used to strengthen composite materials. In addition to its own strength, a high aspect ratio (>20) is also a key factor to obtain high-strength composite materials. The aspect ratio of CNTs is generally >1000. Therefore, through CNT-reinforced composite materials, it can show good mechanical strength and fatigue resistance [10, 40].

The carbon atoms in CNTs are arranged in a six-membered ring network structure, which is very conducive to phonon vibration. Therefore, CNTs have good thermal conductivity. Due to the anisotropy of the structure, the thermal conductivity of CNTs along the length direction is much higher than that in the vertical direction. Theoretically, the thermal conductivity of SWCNTs can reach 10,000 W/mK at room temperature. Due to the presence of impurities, the highest experimental values of SWCNTs and MWCNTs are 3500 and 3000 W/mK, respectively [42–44]. Theoretical calculation and experimental results show that with the increase of CNT diameter, the thermal conductivity of CNTs shows a downward trend (**Figure 2**) [45]. This is because the increase of diameter inevitably increases the defect content, which leads to more phonon scattering.

CNTs are widely used in various electronic devices due to their high conductivity and chemical stability [46]. For SWCNTs, the specific surface area of SWNTs can reach 240–1250 $m^2 \cdot g^{-1}$, which can generate 180 $F \cdot g^{-1}$ specific capacitance, 20 $kW \cdot kg^{-1}$ power density, and 6.5–7 $Wh \cdot kg^{-1}$ energy density. At the same time, high-temperature heat treatment can reduce the electrode impedance and increase the specific capacitance of SWNTs. The increase of capacitance is considered to be caused by the increase of specific surface area and a large number of 3–5 nm pore distribution [47, 48]. For MWCNTs, they usually have a high specific surface area (about 430 $m^2 \cdot g^{-1}$), a specific capacitance of up to 180 $F \cdot g^{-1}$, a power density of 8 $kW \cdot kg^{-1}$, and an energy density of 0.56 $Wh \cdot kg^{-1}$. CNTs of different shapes (such as direct growth, porous, array, and crimp)

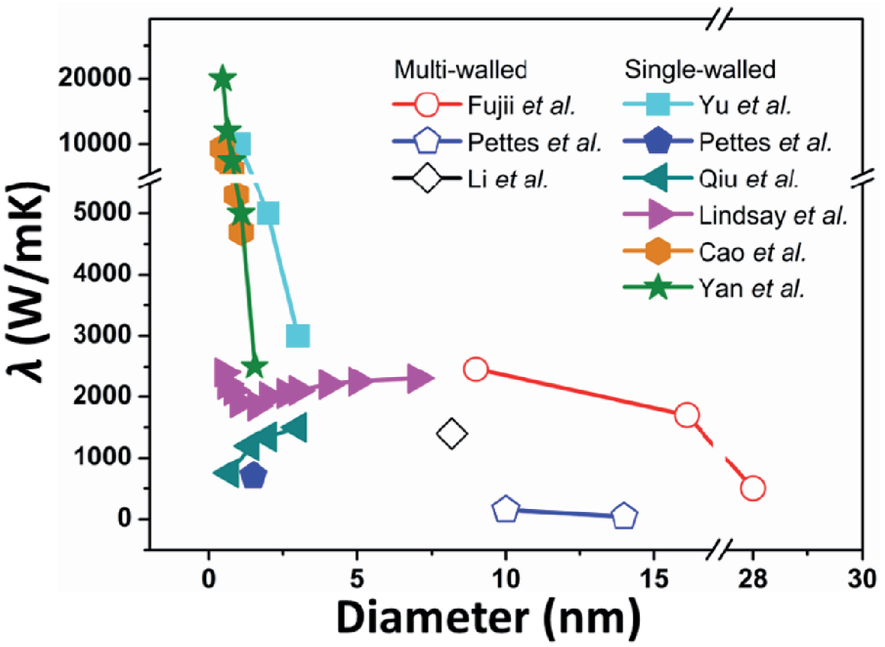

Figure 2.
The relationship between thermal conductivity and diameter of CNTs [45].

have been tested as electrodes. The array CNT is the most suitable electrode because of its small internal resistance, good reaction rate, regular gap structure, and stable conductive channel [49–51].

3. Carbon fibers

Carbon fiber is a kind of fiber material with high strength and high modulus. Its carbon content is more than 90%, and CF with carbon content more than 99% is also called graphite fiber, which is mainly composed of disordered graphite microcrystals stacked along the axial direction of the fiber [52]. CF is not only flexible and acid and alkali resistant but also stronger than steel, which makes it an important material for national defense, military industry, and civil use [53].

CF can be classified into polyacrylonitrile-based (PAN-based) CF, asphalt-based CF, viscose-based CF, and gas-phase growth CF according to the source of precursors [52]. As shown in **Figure 3**, according to the basic morphology, it can be divided into filament CF and short CF, wherein filament CF can be woven into two-dimensional CF fabric and three-dimensional CF fabric. Based on the mechanical properties, it can be divided into general CF and high-performance CF which can also be divided into high-strength type (strength >2000 MPa) and high model type (modulus >300 GPa) CF. With the rapid development of aerospace, automobile manufacturing, and sports facilities, the performance of CF has been increased, and the outputs have been improved continuously. Currently, the largest amount of polyacrylonitrile-based CF is used in the real world [54].

3.1 Fabrication of CFs

The industrial production of CF mainly includes polyacrylonitrile-based CF, asphalt-based CF, and viscose-based CF. Among them, the preparation process of viscose-based CF must be graphitized by high-temperature stretching. Because of its complex equipment and technical difficulties, it has not been effectively developed. The production process of polyacrylonitrile-based CF mainly includes two processes:

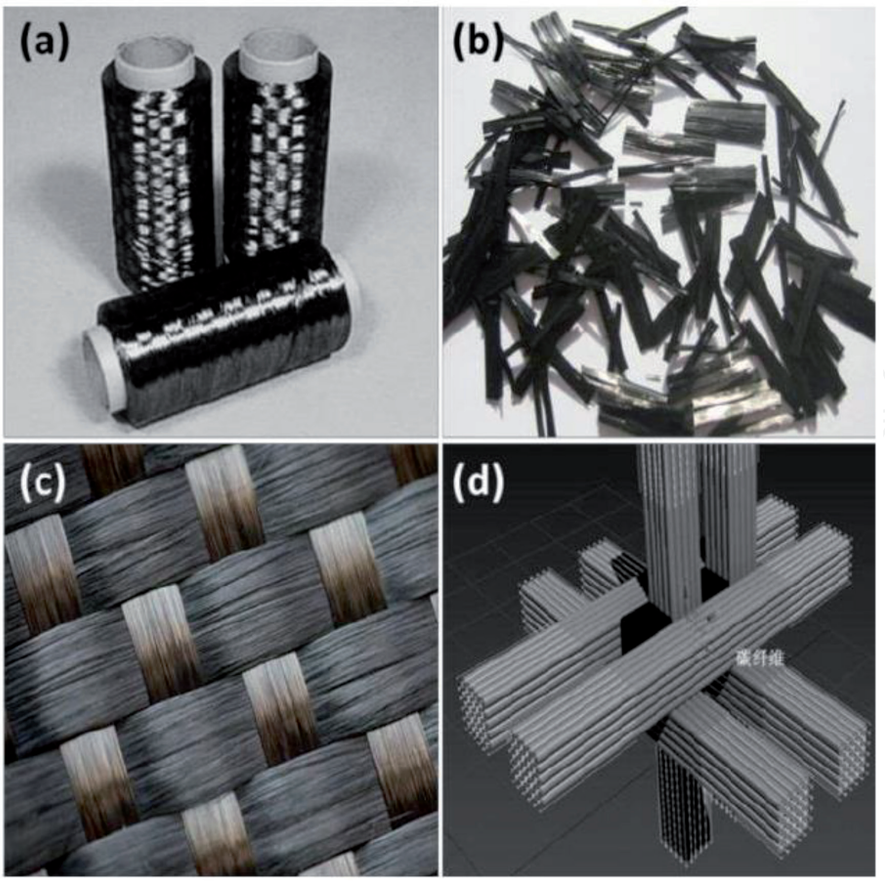

Figure 3.
The pictures of (a) filament CF, (b) short CF, (c) CF cloth, and (d) 3D CF braid.

raw silk production and carbonization. The production process of raw silk mainly consists of polymerization of acrylonitrile monomer, solution defoaming, wire spraying, traction, water washing, oiling, drying, and reeling. Moreover, the carbonization process mainly includes pre-oxidation, low-temperature carbonization, high-temperature carbonization, surface treatment, sizing and drying, winding, and other processes. Note that the pre-oxidation refers to heating the precursor fiber in the air to about 270°C, holding for a period of time, so that the polyacrylonitrile linear polymer will be oxidized, pyrolyzed, cross-linked, and cyclized to form a heat-resistant ladder polymer. In order to prevent melting and deformation of polyacrylonitrile fiber during high-temperature carbonization, the color of polyacrylonitrile fiber gradually changes from white to yellow, then brown, and finally black. The pre-oxidized fiber is carbonized in inert gas with high temperature, and then the cross-linking reaction arises further. With the removal of hydrogen, nitrogen, and oxygen atoms, CF with disordered graphite structure is formed.

The raw material of asphalt-based CF is petroleum asphalt or coal asphalt. The preparation process mainly includes refining, spinning, pre-oxidation, carbonization, or graphitization of asphalt. Among them, mesophase asphalt is a kind of nematic liquid crystal (LC) material composed of disk-shaped or rod-shaped molecules formed by heavy aromatics during heat treatment. The asphalt-based CF prepared by mesophase asphalt is easy to graphitize and usually has a high modulus [52, 55–57].

3.2 Properties of CF

Due to the carbonization and orientation at high temperatures, the carbon atoms of CF are arranged very closely, and the disordered graphite is closely connected. In addition, the diameter of CF is smaller, which can reduce the content of defects, so

it has very high mechanical strength and modulus. The tensile strength and modulus of CF can reach 7 and 700 GPa, which are much higher than those of glass fiber and Kevlar fiber. CF can withstand high temperature above 3000°C without contact with air. Therefore, CF has outstanding heat-resistant performance. The higher is the temperature, the greater is the fiber strength. After graphitization, the density of mesophase asphalt-based CF increases, and the carbon content exceeds 99%. Most of the carbon atoms in the fiber form a large area of graphite sheet structure along the fiber axis by SP^2 hybridization, which is very conducive to the phonon vibration. Therefore, the thermal conductivity of the graphite fiber can reach up to 1000 W/mK [45, 58, 59]. It is worth noting that the electrical properties of CF are not ideal, because of the inherent polycrystalline structure and a large number of grain boundaries inevitably formed during the pyrolysis of organic precursors [21].

4. Graphene-based fibers (GBFs)

Graphene is a two-dimensional (2D) crystalline sheet with a monolayer of carbon atoms densely packed in an SP^2-bonded honeycomb lattice and can be considered as a single layer of the graphitic film in graphite. Thus, graphene is the thinnest nanomaterial known [60, 61]. As shown in **Figure 4**, the length of carbon–carbon bond in graphene is about 0.142 nm; all carbon atoms are connected with three surrounding carbon atoms by σ bond; the remaining P electron orbit is perpendicular to the plane of graphene to form delocalized π bond because π electron can move freely in the plane, rendering graphene holding excellent electrical properties [62, 63].

Since graphene was found in 2004 [61], because of its unique physical and chemical characteristics, such as extraordinary thermal conductivity [64], mechanical strength ($\sigma_{int}^{2D} = 42 \pm 4 (N \cdot m^{-1})$) [65], and fast electron mobility ($\mu \approx 10{,}000$ $cm^2 \cdot V^{-1} \cdot s^{-1}$) [66–70], it has aroused great interest. Due to the oxygen-containing functional groups, graphene materials obtained from chemical methods such as graphene oxide and reduced graphene oxide (rGO) are highly maneuverable and reactive, which further inspires a wide range of research enthusiasm in preparation, chemical modification, and well-controlled assembly of advanced and macroscopic structures for various device applications [71–77]. To this end, graphene-based 3D aerogels (GBAs), 2D membranes (GBMs), and 1D fibers (GBFs) have been developed. Among them, GBAs hold the current world record for the lightest material,

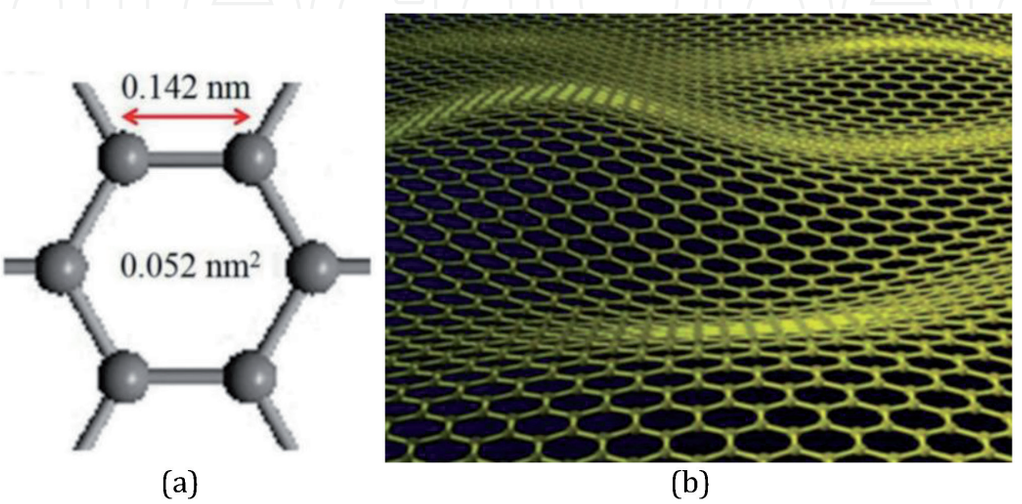

Figure 4.
(a) Schematic diagram of a honeycomb crystal lattice of graphene, and (b) a single-layer suspended graphene sheet exhibits intrinsic microscopic roughening.

with a density of 0.16 mg · cm^{-3} [78], and have demonstrated good capability in the removal of spilled oils [78, 79]. GBMs, which are usually fabricated by infiltration or CVD, have also found to have various applications in the field of energy storage and conversion [80]. Compared with GBAs and GBMs, GBFs possess not only outstanding mechanical property and high conductivity but also good valuable flexibility that can be curved, knotted, and even woven into flexible conductive fabric, which are considered capable of improving the practical applications of GBFs. The development of high-performance GBFs could inspire more engineering applications of graphene. However, assembling microscopic graphene sheets into 1D fiber remains as an unusual challenge because of the irregular shape and size and the movable stacked layers of graphene sheets compared with the highly tangled CNT assemblies [63]. Nevertheless, the assembly of graphene sheets into macroscopic fibers has attracted wide interest due to the lightweight, lower cost, shareability, ease of functionalization, and practical importance of GBFs in contrast to CNTs and CF. Beyond that, 1D GFs with mechanical flexibility is particularly important for wearable textile devices and can serve as the building blocks for constructing 2D and 3D macroscopic architectures for various applications.

4.1 Fabrication of GBFs

At present, the manufacturing methods of GBFs are mainly influenced by traditional synthetic fiber production methods, including melt spinning and solution spinning [63]. However, due to the high-temperature stability of graphene, its melting temperature is even higher than that of fullerene and carbon nanotubes. Therefore, melt spinning is not the choice for manufacturing GBFs, while solution spinning is [81, 82]. Solution spinning mainly includes wet spinning, dry jet wet spinning, and dry spinning. In addition to these traditional solution spinning methods, some new methods, including electrophoresis, template hydrothermal method, and chemical vapor deposition-assisted assembly, have been developed recently. In this part, the common methods of preparing GBFs will be introduced in detail.

4.1.1 Wet spinning

Wet spinning is one of the main methods to prepare chemical fiber. The important step is to prepare a spinning solution. Because graphene is not easily dispersed in water or other organic solvents, it is difficult to prepare a spinning solution, so it is not possible to prepare fibers from graphene by wet spinning [83–85]. As an important precursor of graphene, graphene oxide can be well dispersed in polar solvents (such as water), so it is expected to prepare fibers by wet spinning [86]. The steps of preparing GBFs by wet spinning are as follows: first, GO dispersions are injected into a stable aqueous solution to form GO spinning dope and then injected into the coagulation bath to form a gel-like fiber to prepare GO dope. After solidification for a period of time, GO fiber can be obtained by extracting colloidal fiber and drying, and then GO fiber can be reduced to produce GBFs, as shown in **Figure 5**. An rGO fiber can be further produced by reducing the GO fiber when needed [86, 87]. To ensure uniform and continuous formation of gelatinous fibers, the fibers after solidification should be kept at a certain speed. They can be drawn through a rotating bath or using a collecting unit, as shown in **Figure 5**. The highest strength rGO fiber is made by the method shown in **Figure 5a**. This method includes an easy spin of a small amount of fiber, but it lacks accurate control of fiber moving speed. In contrast, the method shown in **Figure 5b** can provide constant traction and determined moving speed to synthesize fibers, so the method is more suitable for producing fibers with accurate tensile ratio and good scalability [88].

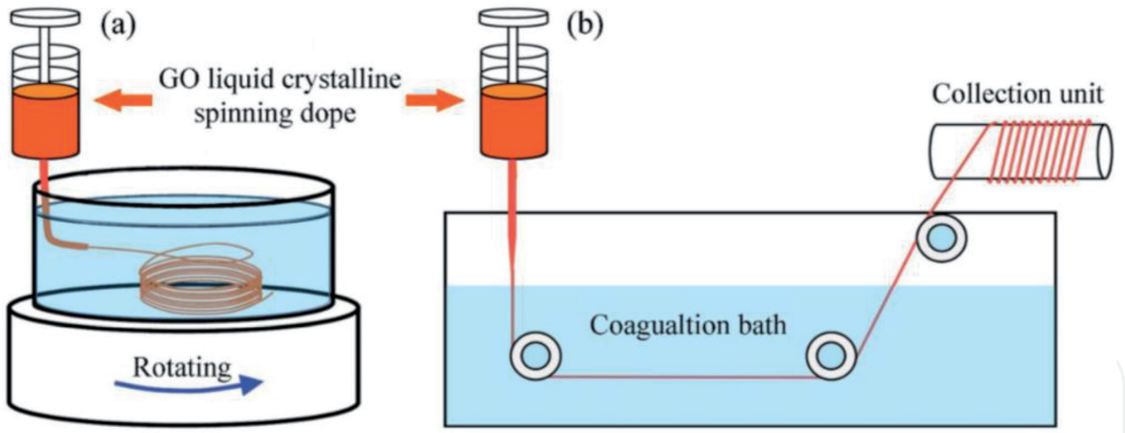

Figure 5.
(a) The synthesis of graphene oxide fiber by wet spinning in rotating coagulation bath and (b) collection unit [86, 87].

Zhen et al. prepared liquid crystal GO aqueous solution for the first time in 2011, taking NaOH/methanol solution as coagulation bath, obtaining GO fiber through wet spinning, and then reducing GO fiber in hydroiodic acid to produce GBFs. This method can make GO sheets form liquid crystals, which can enhance the strength and flexibility of GBFs. The tensile strength of the fiber is 140 MPa, and the conductivity is 2.5×10^4 S · m^{-1} [86]. Then, Zhen et al. further tried to increase the lamella of the raw material GO, using N,N-dimethylformamide (DMF) as the solvent, acetone, and ethyl acetate mixture as the coagulation bath. After that, the mechanical ability of GBFs was improved by spinning drafting and high-temperature treatment at 3000°C, making its strength reach 1.45 GPa [89]. On the other hand, the conductivity of GBFs can be improved by ion doping, and the conductivity of potassium doped GBFs can reach 2.24 × 107 S · m^{-1} [90]. In addition, Shaohua et al. prepared non-liquid crystal GO aqueous solution to achieve a high concentration of spinning solution to improve the fiber yield. The concentration of a spinning solution can reach 2%, and then GBFs were obtained through a similar wet spinning process and reduction by hydrocodone. The mechanical and electrical properties of the fiber were 208 MPa and 1.53 × 103 S · m^{-1} [91], respectively.

In addition to GBFs, graphene composite fibers can also be prepared by wet spinning, so as to effectively improve the fiber performance and expand the application field. Conducting polymer monomers are polymerized in situ during spinning to prepare composite fibers [92, 93], or oxides or other materials are added directly into the spinning solution to increase the capacity of fiber-shaped supercapacitors [94, 95]. Wujun et al. used GO to disperse the water-insoluble activated carbon in the aqueous solution, spinning and reducing to obtain graphene/activated carbon composite fiber. The fiber has a specific surface area of 1476.5 m^2 · g^{-1} and a capacity of 43.8 F · g^{-1} [96]. Similarly, the graphene/manganese dioxide composite fiber can be spun by a similar process, and the capacity of the supercapacitor can reach 66.1 F · cm^{-3} [97]. In addition to inorganic materials, GO and polyvinyl alcohol (PVA) also have good compatibility. Adding sodium hydroxide to non-liquid crystal GO aqueous solution for a pH = 11. Then, adding PVA can significantly increase the affinity between fiber and electrolyte [98]. Similarly, the surface of the fiber with a large number of hydroxyl groups can significantly increase the hydrophilicity and strength of the fiber, which is caused by a large number of oxygen-containing functional groups on its surface [99]. Mochen et al. developed a method to improve the strength of graphene fiber. They spun GO and phenolic resin together. After carbonization under the condition on 1000°C, the C–C covalent bond was formed between graphene sheets, and the fiber strength reached 1.45 GPa [100].

The tensile strength and elongation at break of graphene fiber with 10% phenolic resin are 1.45 GPa and 1.8%, respectively, which are better than most GBFs reported before. The increase of strength, toughness, and elongation can be attributed to the formation of a C–C bond between the graphene sheet and phenolic carbon, which provides sliding space for the graphene sheet before fracture. Yang et al. developed a simple but effective method for continuous manufacturing of neat, morphologically defined, graphene-based hollow fibers (HFs) with coaxial capillary spinning strategy. As shown in **Figure 6**, the preparation method of GO-HFs is to use coaxial capillary spinneret to spray silk in 3 mol · L^{-1} KCl methanol solution and use compressed air to replace the internal fluid of KCl/methanol solution to successfully prepare GO-HFs with necklace structure (nGO-HF). Experiments show that nGO-HF has a large elongation of about 6% when it breaks, which indicates that nGO-HF has a strong ability to bear compression, which is caused by the elastic deformation of hollow microspheres [101]. Therefore, the physical properties of GBFs can be controlled by adjusting the spinning conditions.

4.1.2 Dry spinning

In the dry spinning of GBFs, GO dispersion (mainly dispersed in water) is also used as a spinning assistant rather than a coagulation bath. Instead, the GO dispersion is injected and sealed in a pipe, and the GO dispersion is precipitated in the form of gel state fiber at high temperature by heating or chemical reduction, and then dried rGO fibers can be obtained by further solvent removal. GO dispersions are considered to be colloids with large-size dispersants [102–104]. The study of Dong et al. and Yu et al. shows that high temperature can promote the rapid movement of GO dispersant and increase the possibility of collision and precipitation of GO plate. At the same time, high temperature or chemical reduction can also separate the

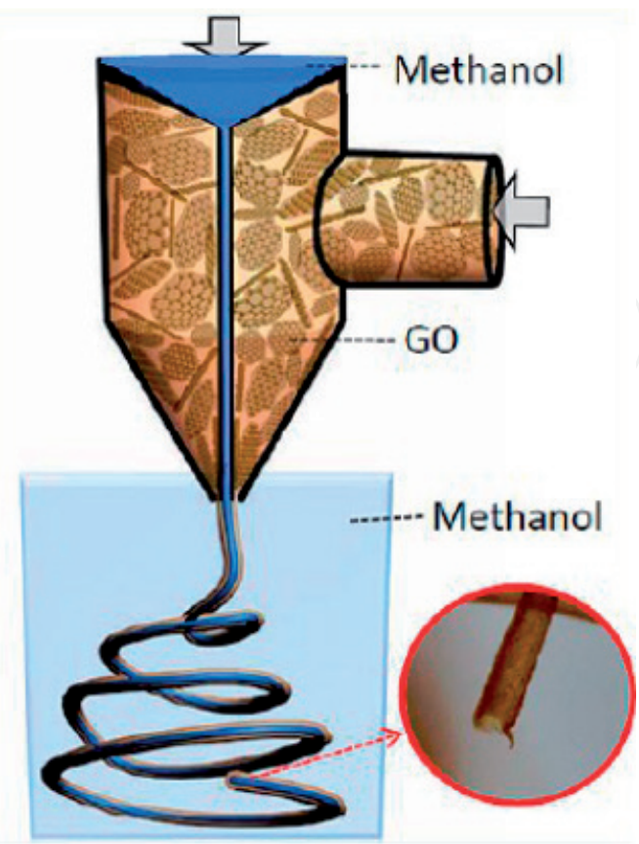

Figure 6.
Schematic of the setup that used a dual-capillary spinneret to directly spin GO-HFs [102].

oxygen-containing groups in GO and reduce the zeta absolute potential of GO dispersion. Finally, due to the lack of sufficient electrostatic repulsion, GO sheets' precipitate is assembled into fibers. The fibers in the gelatinous state expand in the solvent, but the diameter of the fibers can be reduced by about 80% after drying [105, 106].

In the process of dry spinning, the precipitate of GO sheet under the condition of 220–230°C is actually a solvothermal process (the water is used as the solvent to disperse GO). The process flow is shown in **Figure 7** [107], and the fibers made in this way are actually rGO fibers. It is reported that 27% of oxygen in GO can be removed at 180°C and most hydroxyl, epoxy, and carboxyl groups begin to separate at 200°C [108, 109]. Therefore, GBFs synthesized by the hydrothermal method has considerable conductivity, without post-reduction treatment [105, 110]. In addition to the hydrothermal method, Jihao et al. also use the chemical reduction method of CO to produce rGO fiber. First, the GO and vitamin C (VC) solution was injected into the polypropylene (PP) tube, then heated to 80°C, and kept for 1 h, while GO was reduced and assembled into gel-like rGO fibers. After extraction and drying, the fiber diameter decreased by 95–97%, which was due to the shrinkage of the fiber due to the removal of moisture. Finally, the conductivity of the rGO fiber is about 8 $S \cdot cm^{-1}$ [111].

In the dry spinning process, GO dispersion does not necessarily exist in the form of liquid crystal [106]. The randomly dispersed low-concentration GO dopes (8 $mg \cdot ML^{-1}$) composed of small-diameter GO (d = 0.5–4 μm) can also be used for the synthesis of GBFs [112, 113]. Compared with the wet spinning method, the preparation of graphene fiber by dry spinning does not need other auxiliary reagents, only needs high-temperature reduction or chemical reaction to get GBFs, and can get any shape of GBFs by pre-setting template, even hollow structure GBFs [105, 106, 112]. It is worth noting that after reduction, the strength of GO fiber obtained by dry spinning is lower than that by wet spinning, but its toughness is as high as 19.12 $MJ \cdot m^{-3}$, which is expected to become a green processing method of GBFs in the future [107].

4.1.3 Dry jet wet spinning

Dry jet wet spinning is another important spinning method of conventional synthetic fiber. The results show that PAN-based carbon fibers can be spun with high concentration coating by this method and the mechanical properties of the fiber are better than that of wet spinning [52, 114]. Shayan et al. use dry jet wet spinning to improve the strength of the fiber. The existence of the air layer effectively reduces the speed gradient of the spinning liquid from the spinneret to the coagulation bath, so that the fiber has a better arrangement. However, if the air layer is too long, it will affect the tensile property of the fiber and control the diameter of the needle and the distance of the air layer. Then, the high-strength GBFs with circular cross section can be spun (**Figure 8a**) [115].

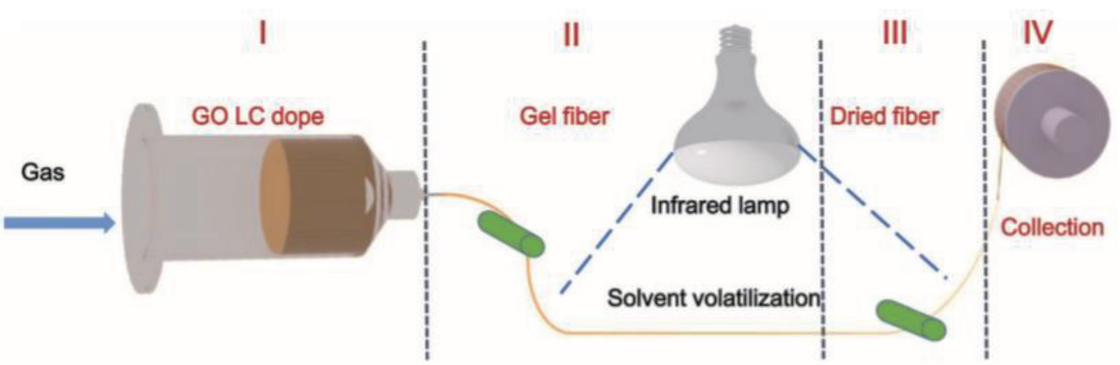

Figure 7.
Schematic illustration of the dry spinning process with a concentrated organic dispersion of GO [108].

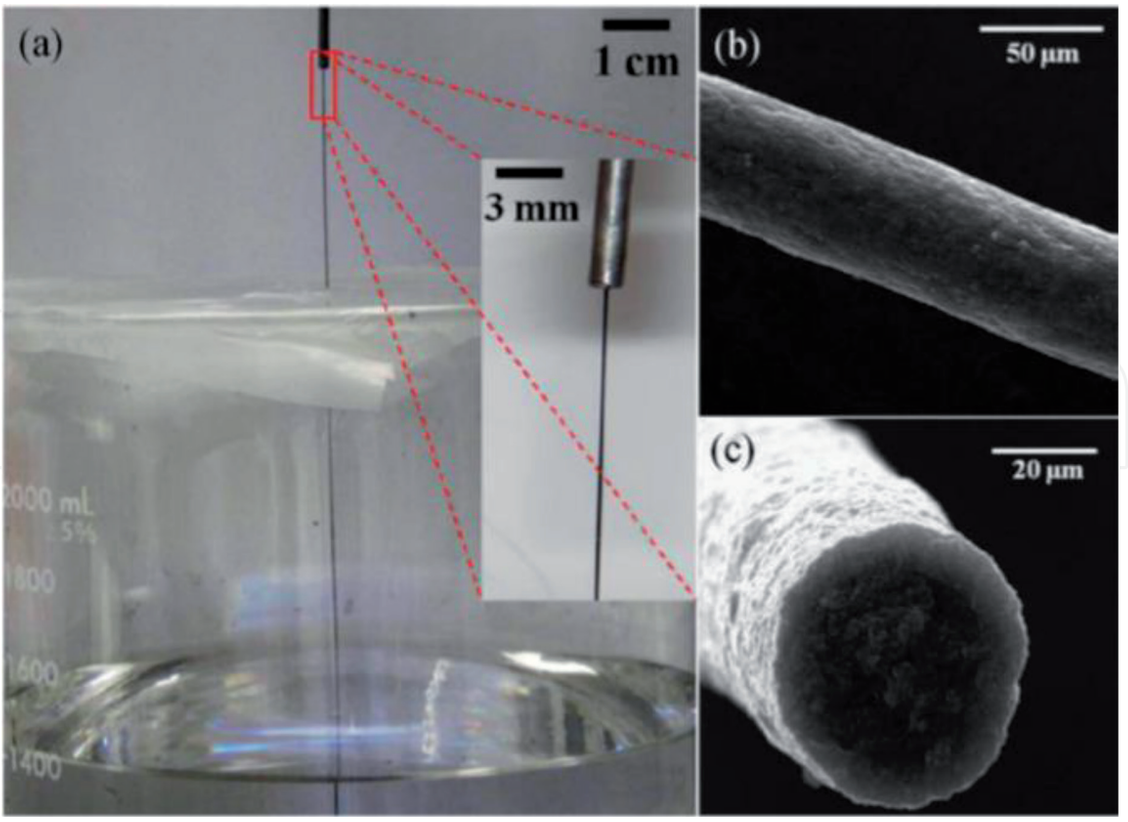

Figure 8.
(a) A digital photo showing the setup for dry jet wet spinning of GBFs [115]. (b) and (c) Surface and cross-sectional images of a GBFs [103].

Figure 8b and **c** shows the surface and cross-sectional images of dry jet wet spinning fiber, which indicates that the GBFs with smooth surface and circular cross section can be produced by dry jet wet spinning with proper solvent coalescent pair (chlorosulfonic acid and diethyl ether), which is not realized in both wet spinning and dry spinning.

4.1.4 Chemical vapor deposition-assisted assembly

In the production of graphene made by chemical vapor deposition, the composition of graphene can be easily changed by changing the composition of the gas phase. Xinming et al. reported in 2011 a method of self-assembly of two-dimensional CVD grown films into one-dimensional GBFs in ethanol, acetone, and other organic solvents through the change of surface tension. The resulting fibers have a high conductivity of about 1000 $S \cdot m^{-1}$ [116]. Seyed et al. reported another method of film assembly. They first scraped and coated the GO dispersion into multiple film strips, dried and twisted it to get GO fiber, and then put it through thermal reduction to get GBFs. The GO fiber made by this method has high elongation at break (8.3–78.3%) and excellent fracture toughness (1.3–17.4 $J \cdot m^{-3}$), but its strength is low (9.7–85.9 MPa) due to many defects in the fiber section [117]. Jiali et al. also developed a method for preparing GBFs by film shrinkage, as shown in **Figure 9**. First, graphene was produced on copper foil by CVD with methane as a carbon source. In order to obtain a complete and independent graphene film, a layer of polymethyl methacrylate (PMMA) is spin-coated on the surface of graphene. The copper foil is etched with 1 M ammonium persulfate solution, and the PMMA layer is washed off with acetone to obtain the laminated graphene film. Second, the film is pulled out of the solution with tweezers to shrink to form GBFs with uniform diameter [118]. The graphene film can be directly used to prepare GBFs by film

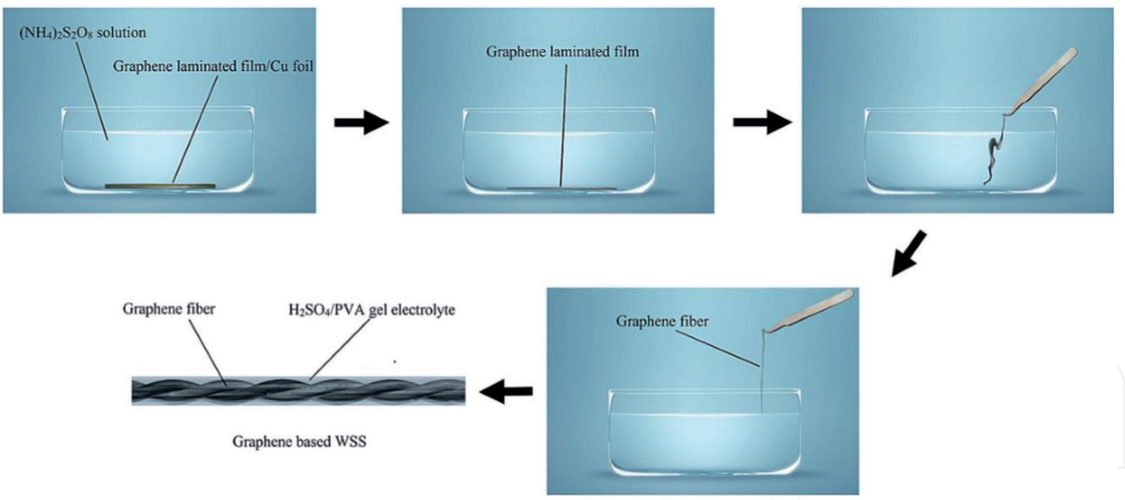

Figure 9.
Schematic illustration of GBFs prepared by film assembly [118].

shrinkage method, and the obtained fiber generally has more pores. However, the CVD method needs a lot of instrument investment and strict gas conditions, and the cost is high, so it is difficult to promote.

4.1.5 Templated hydrothermal method

Zelin et al. reported a template hydrothermal method to prepare GBFs. GO dispersion was injected into the stripping pipe, sealed at both ends, and then heat-treated in water at 230°C for 2 h to form continuous GBFs. The structure of GBFs can be adjusted by controlling the concentration of GO dispersion and the inner diameter of a glass tube. The graphene fiber has a porous structure, has a density of only 0.23 g · cm^{-3}, and has a good flexibility [105]. Yunming et al. used a simple low-temperature-induced self-assembly method to synthesize GBFs. They mixed GO and ascorbic acid evenly and sealed them in a specific straight glass tube. They carried out the hydrothermal reaction at 90°C and 120°C, respectively, until the fiber was completely formed and then obtained GBFs with layered porous structure. Its conductivity can reach 1.3 × 10^4 S · m^{-1}. After heating, it has excellent mechanical properties and can be easily woven into the spinning products [119]. Lizhi et al. further developed on the basis of previous methods, and the specific preparation process is shown in **Figure 10**.

First, the dispersion of GO is sprayed into liquid nitrogen through a spout to prepare a layer bridging GO dispersion - interconnected graphene oxide ribbons (IGOR). Then, a certain concentration of GO dispersion is uniformly mixed with IGOR dispersion and injected into a quartz capillary with an inner diameter of 0.4 mm. The two ends are sealed, heated at 230°C for 2 h, and finally dried in air for 12 h. The GBFs show higher strength and toughness [120].

In order to increase the length of GBFs prepared by the hydrothermal method, Dingshan et al. improved the above methods. The authors replaced the brittle glass tube with the flexible and high-temperature-resistant fused silica capillary column, injected the GO dispersion containing ethylenediamine into it, and sealed it. After that, they put it in the furnace at 220°C for 6 h, extruded it with nitrogen to form the fiber, dried it, and collected the long enough GBFs [106]. Although the GBFs with porous structure can be prepared by the hydrothermal method, it is difficult to achieve continuous production because of the need of closed space and long reaction time.

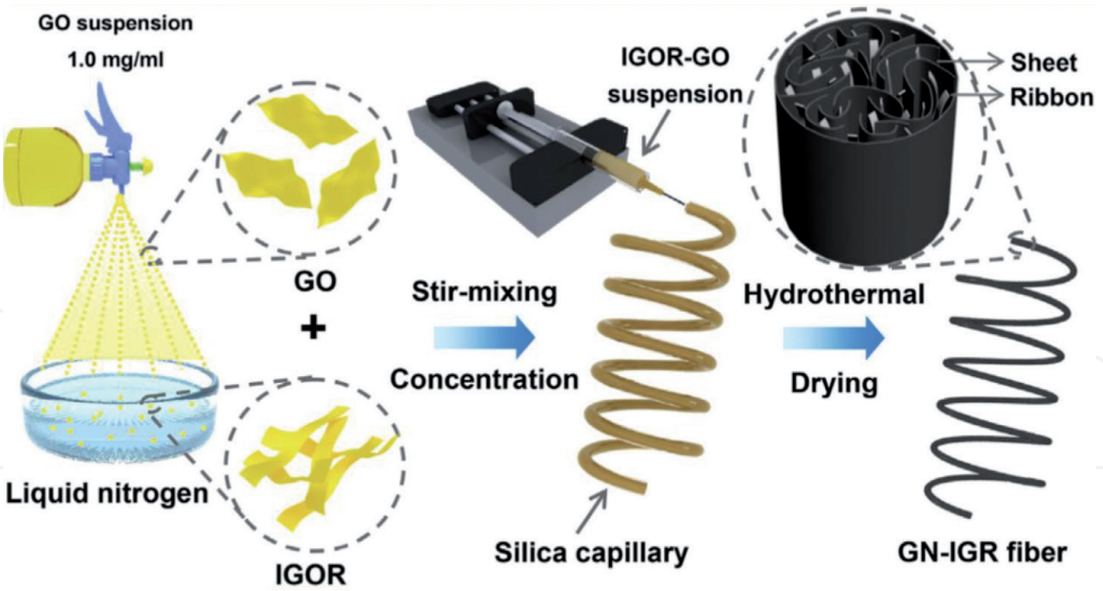

Figure 10.
Schematic illustration of graphene hybrid fibers prepared by hydrothermal method [120].

4.1.6 Conductive substrate-assisted spontaneous reduction and assembly

The conductive substrate-induced spontaneous reduction and self-assembly of GO generally proceeds by putting metal substrates (e.g., Al, Fe, Cu) into GO solution for GBF preparation. As shown in **Figure 11**, Junjie et al. take copper wire as the substrate and adopt the three-electrode method to make the GO sheet continuously deposit on the surface of copper wire under the double induction of electrochemistry and template. Both GO and copper are simultaneously restored. Then, they etch and remove the copper wire in the $FeCl_3$ solution to obtain the graphene hollow fiber with an oriented structure. The controllable preparation of the hollow fiber can be realized by controlling the diameter, length of the substrate, and the time of electrochemical deposition. The graphene hollow fiber has excellent flexibility and conductivity and can be used as the electrode material of supercapacitor [121].

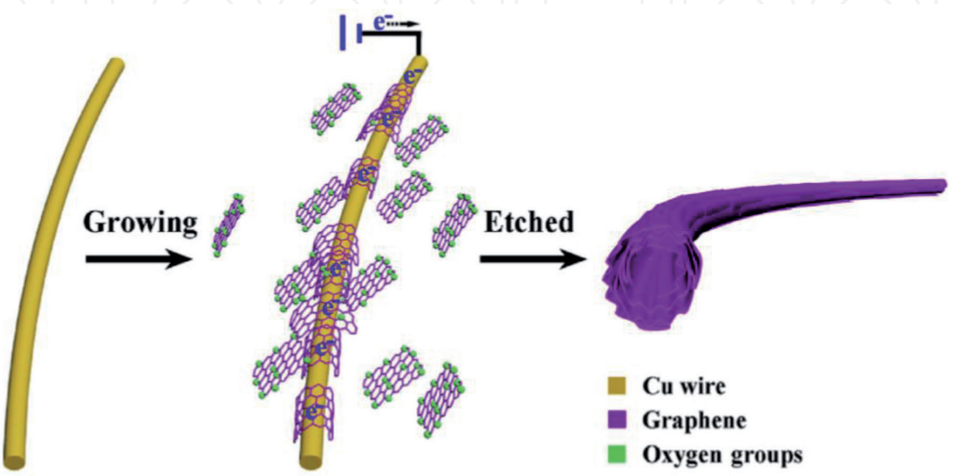

Figure 11.
Scheme of spontaneous reduction and assembly of graphene hollow fiber on active metals substrates [121].

4.1.7 Electrophoresis self-assembly method

The electrophoretic phenomenon occurs in a colloidal solution because charged particles can move under the action of electric field. Lianlian et al. developed a method for preparing GBFs with electrophoretic self-assembly. The graphite probe was used as a positive electrode to invade the GO dispersion. Under constant potential, the graphite probe was extracted slowly and uniformly, and self-assembled GO fibers were formed at the tail of the cathode. After drying and heating, GBFs with a smooth surface and circular cross section can be obtained [122]. Because the electrode moving speed is only 0.1 mm · mm^{-1}, it takes 1 week to get 1-m-long fiber. The yield of GBFs obtained by this method is too low to scale production.

4.2 Applications of GBFs

Thanks to graphene's superior electrical, mechanical, and thermal properties and good flexibility, GBFs have great potential in sensor, energy storage, energy conversion, and other fields.

4.2.1 Sensor

With the continuous development of flexible equipment, intelligent devices, including electricity, humidity, force, and temperature, can rapidly make structural changes in the environment and be increasingly concerned by people. The GBFs shows excellent performance in this regard.

Zhao et al. successfully developed a graphene-based multifunctional optical fiber sensor, which can respond to three different stimulations. They deposited GCN on GF (GF and GCN) and twisted it with another GF to form a double helix GBFs. In the twisted structure, the contact interface of the two fibers has a sandwich-like graphene/GCN/graphene structure. Under different external voltage controls, GF and GCN can show three different stimulus modes. Each mode can respond to temperature fluctuation, mechanical interaction, and humidity change and has a high sensitivity to specific stimulation [123]. Yanhong and his team electroplated polypyrrole on half of the surface of GBFs, which changes the current transmission rate on both sides of the fiber. With different types of current, the fiber has different bending states. The prepared electric GBFs are expected to be applied in the multi-arm tweezers and mesh driver [124]. Chunfei et al. used twisted GBFs to realize temperature sensing. With the increase of temperature, the fiber resistance decreases. This is mainly due to the transition of semiconductor characteristics between graphene sheets. The fiber has similar sensing characteristics for temperature under different stretching conditions and has a wide application prospect [125].

In addition, GO fiber is partially restored by laser method, which is sensitive to humidity. By changing the position, the fiber can be transformed into various shapes. Taking advantage of the hydrophilic characteristics of GO in a humid environment, the distance between sheets is increased, while graphene is non-hydrophilic. Hence, the bending degree of the fiber changes with the humidity. Meanwhile, the fiber is woven into fabric shape, which still has sensitive response performance [126]. After twisting the spinning GO fiber, the twisted fiber will rotate repeatedly as the humidity changes periodically. When the humidity increase, a large number of oxygen-containing functional groups on the surface of GO will absorb water, and the distance between layers will increase. Otherwise, the distance between layers will decrease. A magnet is added at the lower end of the fiber to prepare a humidity sensing electric motor. The speed of the motor reaches 5190 r · min^{-1}. The motor can convert the change of environmental humidity into electric energy and realize the collection of energy [127].

The GBFs and the GBFs coated with a layer of carbon nitride on the surface are wound together. The middle carbon nitride layer is equivalent to a buffer layer. Its conductivity is related to the layer spacing. With the pressure increase, the distance decreases and the conductivity is, in turn, to increase, which can realize the stress sensing [123].

4.2.2 Energy storage

4.2.2.1 Lithium-ion batteries

With the development of science and society, a portable energy storage device is becoming smaller and more flexible. Lithium-ion batteries are a new type of energy storage device, which has the advantages of high energy density, environmental friendliness, long cycle life, and high working voltage. However, the traditional LIBs cannot meet the needs of wearable electronic devices due to its large usage, rigidity, and weight. Therefore, it is necessary to develop new batteries with small volume, lightweight, and high flexibility. GBFs maintain the unique characteristics of the graphene nanosheet. When GBFs are used in the fiber lithium battery, it can realize the series connection with flexible electronic devices and drive them to work stably, achieving high energy density and holding a good commercial prospect [128, 129].

Jung et al. of the Korea Institute of Chemistry used pure GBFs as the negative electrode material of lithium-ion batteries. The battery circulates 100 times in the range of 0.005–3 V under the current density of 100 $mA \cdot g^{-1}$, and the capacity is still 224 $mAh \cdot g^{-1}$ [130]. Minsu et al. obtained hollow GBFs by coaxial spinning and increased specific surface area and active site, and its capacity remained 196 $mAh \cdot g^{-1}$ in the range of 0.005–1.5 V for 100 cycles under the current density of 0.2C [131]. Due to the low capacity of pure GBF battery, Jong et al. added MnO_2 active material in graphene; the addition of MnO_2 increased the distance between graphene sheets and gave lithium-ion fast transfer channel. Moreover, the battery made by MnO_2 coating of graphene has good cycle stability, and the cycle capacity of 100 times remained 560 $mA \cdot g^{-1}$. Minsu et al. filled the inner space with Si/Ag nanoparticles, and the outer graphene well controlled the volume expansion of the inner silicon during charging and discharging, providing a smooth electronic channel. Compared with the simple mixing process, it has better cycle stability and rate performance, and the capacity of 100 cycles remains 766 $mAh \cdot g^{-1}$ [131].

The GBFs prepared by the above method have low strength, and it is difficult to form a macroscopical fiber battery. In one report, a fiber battery electrode comprised of 2D/2D layered titania sheets/rGO sheets (titania/rGO) composites was prepared through wet spinning method [132]. By assembling the cathode of titania/rGO fiber with the anode of lithium wire in parallel, a fiber-shaped half-cell was fabricated. This hybridized fiber electrode had an ordered stacking structure, high linear density of active materials, and abundance of exposed active sites, which endows the fiber electrode with prominent mechanical flexibility combined with excellent battery performances of high linear capacity of 168 $mAh \cdot g^{-1}$, good rate capability, and outstanding cyclic behavior. Woon et al. used wet spinning to construct graphene/carbon tube/sulfur electrode as positive material of Li-S battery. Graphene has high conductivity and can transfer electrons rapidly. Meanwhile, GO fiber as a matrix can obtain light fiber with certain mechanical strength for wearable equipment, as shown in **Figure 12a** and **b** [133].

Compared with wet spinning, the diameter of the nanofiber film obtained by electrospinning is smaller. As the electrode material of lithium battery, it can significantly reduce the migration distance of lithium-ion and increase the specific surface area of the electrode material and improve the electrochemical performance

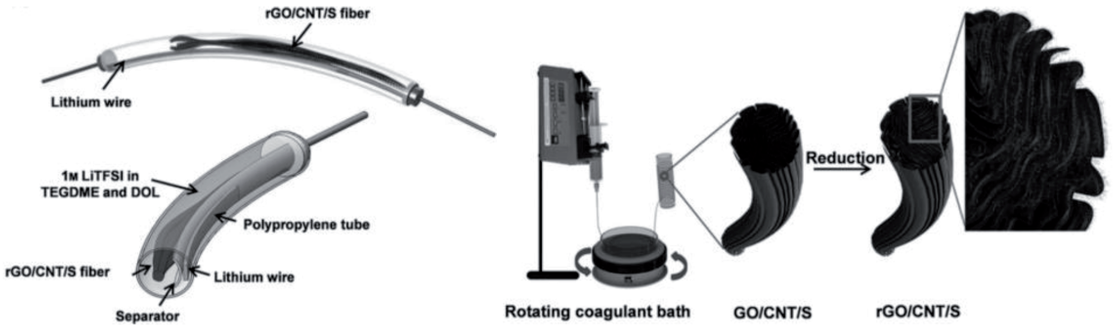

Figure 12.
(a) Schematic of fiber-shaped lithium-ion battery. (b) Schematic illustration of synthetic route of rGO/CNTs/S fiber [133].

of the battery [134–136]. Xiaoxin et al. obtained the Si-graphene-C structure which is similar to the coronary artery based on bionics. Graphene can effectively control the volume expansion of Si, and high conductivity is also conducive to the rapid transfer of ions. Meanwhile, the inclusion of graphene also avoids direct contact between Si and electrolyte and avoids the formation of a large number of SEI films. After 200 cycles, the capacity retention rate is still 86.5% [137]. Jian et al. continued to wrap a layer of graphene outside SnO_2 and GO nanofibers with a double-layer protection method to inhibit the volume expansion and agglomeration of active materials. This method is applicable to almost all oxide and graphene nanofiber electrodes obtained by electrospinning, with good universality [138].

At present, there are few researches on the application of GBFs in LIB and the assembly of woven fiber batteries. Compared with the traditional button batteries, the assembly process of GBFs is relatively complex, so it is unable to achieve continuous production.

4.2.2.2 Supercapacitor

In addition to the application in LIB, GBFs are also widely used in the field of supercapacitors. Supercapacitor, also known as a double electric layer capacitor or electrochemical capacitor, is a new energy storage device that uses the rapid adsorption–desorption of electrolyte ions with electrode materials or the reversible oxidation–reduction reaction on the surface of electrode materials to realize electric energy storage [139, 140]. With the continuous development of wearable devices, flexible supercapacitors have become the preferred energy source for various electronic devices due to their fast charge and discharge ability and long cycle life. Among them, fiber supercapacitors have attracted much attention due to their lightweight, small size, high flexibility, and good wearability. GBFs have excellent conductivity and super high specific surface area, so it has been widely used in the field of fiber supercapacitor [141].

Chen et al. prepared pure GBFs with a non-liquid crystal method and further assembled the fibers into flexible supercapacitors. The capacitance of the supercapacitor is 39.1 $F \cdot g^{-1}$ when the current density is 0.2 $A \cdot g^{-1}$. At the same time, it is found that the electrochemical performance of GBFs can be greatly improved by immersing it into 6 M KOH for 10 min before the electrochemical performance test. At the current density of 0.2 $A \cdot g^{-1}$, the specific capacitance is 185 $F \cdot g^{-1}$ (226 $F \cdot cm^{-3}$), and the energy density is 5.76 $Wh \cdot kg^{-1}$ (power density is 47.3 $W \cdot kg^{-1}$) [91]. The capacitor has good toughness and can be woven into fabric and light LED after charging. Hu and Zhao integrated two electrodes (the upper and

lower part of rGO) and separator (the middle part of GO) into the GO optical fiber, as shown in **Figure 13a**, and made a kind of all-in-one fiber graphene supercapacitor (rGO-GO-rGO) without any adhesive. The diameter of the rGO-GO-rGO fiber is 50 μm, and the rGO part is about 1/4 of the fiber width. The rGO-GO-rGO fiber supercapacitor shows remarkable mechanical flexibility, which can bend to various curvature while maintaining high capacitance (**Figure 13b**) [142, 143].

At present, the specific capacitance of pure GBFs is far less than the theoretical capacitance of graphene. How to improve the capacitance of GBFs is still a big challenge. Currently, an effective method that has been proven and widely used is the hybridization strategy, including doping and compounding with other substances.

Doping increases the active region on the surface of graphene and further improves its catalytic activity for a redox reaction. Among all kinds of atom doping, nitrogen atom doping is the most common. Doping nitrogen atoms with extra valence electrons into graphene will introduce new energy into the low energy region of the carbon conduction band. The introduction to this new energy can improve the catalytic activity and electrochemical performance of graphene materials. Yunzhen et al. extruded the GO dispersion into the substrate of hydroxylamine ethanol solution as a network, dried it, and heat it to obtain the nitrogen-doped rGO network fabric. Then, the PT foil was used as the collector to assemble the supercapacitor. The specific capacity was 188 $F \cdot g^{-1}$ when the scanning rate was 5 $mV \cdot s^{-1}$ in 25% KOH electrolyte. When the scanning rate was increased to 1 and 10 $V \cdot s^{-1}$, the specific capacity was kept at 74.2 and 48.4%, respectively, showing very excellent rate performance [144]. Guan et al. constructed nitrogen-doped porous GBF supercapacitors with high energy density output, large-scale weaving, and flexible wearable application prospects by means of self-assembly of the liquid–liquid interface and molecular functional doping pore formation in the micro-reaction system. The area-specific capacitance of the fiber supercapacitor prepared by this method is as high as 1132 $mF \cdot cm^{-2}$, which has excellent cycle stability and bending durability [145].

Graphene can be compounded with other carbon nanomaterials, conducting polymers, metal oxides/sulfides, and other materials to form graphene composite fibers. The high specific capacitance of the additives can be used to improve the electrochemical performance of the composite fibers.

Yu et al. constructed a graphene/CNT composite fiber. Due to the high conductivity of CNTs, the conductivity of the composite fiber can reach 102 $S \cdot cm^{-1}$, and the specific surface area can reach 396 $m^2 \cdot g^{-1}$. The volume-specific capacitance of the fiber electrode is 305 $F \cdot cm^{-3}$, and the mass-specific capacitance is 508 $F \cdot g^{-1}$ [106]. Yuning et al. mixed GO and pyrrole monomers as spinning solution and extruded

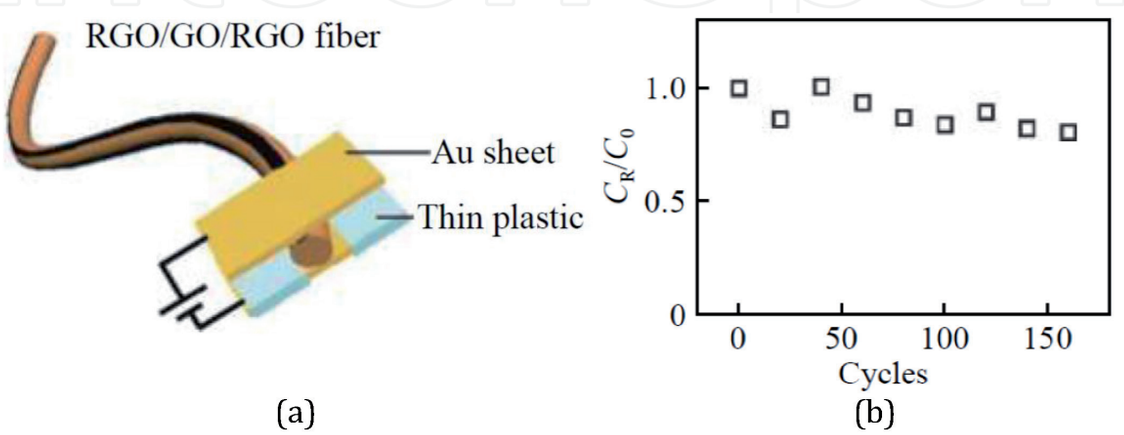

Figure 13.
(a) Scheme of supercapacitor supported by two electrodes. (b) Capacity decrease with increasing bending cycles [142].

them into $FeCl_3$ solution to solidify and polymerize pyrrole in situ, and the PPy/GO composite fiber was obtained after reduction by hydroiodic acid. The fiber has a skin core structure, and its capacitance performance is greatly improved compared with pure rGO fiber. The area-specific capacitance is 107.2 mF · cm^{-2} (73.4 F · g^{-1}), and the energy density is between 6.6 and 9.7 μ Wh · cm^{-2} [146]. Bingjie et al. synthesized the graphene/molybdenum disulfide composite fiber electrode with the one-step hydrothermal method. The electrode has a new intercalation nanostructure, which effectively combines the excellent conductivity of the graphene sheet layer with the high pseudocapacitance of molybdenum disulfide. The final assembled fiber-like super electric container shows a volume-specific capacitance of up to 368 F · cm^{-3} [147]. Qiuyan et al. overcame the problem of poor interaction between MXene layers and prepared MXene/graphene composite fiber. The orientation distribution of MXene sheets among GO liquid crystal templates realized high load (95 w/w%). The composite fiber shows excellent conductivity (2.9 × 10^4 S · m^{-1}) and ultrahigh-volume-specific capacitance (586.4 F · cm^{-3}), far exceeding the value of pure GBFs [148].

In addition, the structure optimization of GBFs is also an effective way to improve the performance of GBF supercapacitor, which mainly lies in the improvement of specific surface area and the regulation of the layer arrangement structure. The porous GO fiber reported by Seyed et al. in 2014 was transformed into porous rGO fiber after thermal reduction at 220°C, as shown in **Figure 14**.

The specific surface area of the fiber is 2210 m^2 · g^{-1}, and the conductivity is about 25 S · cm^{-1}, and the specific capacity of the fiber is 409 F · g^{-1} when the current density is 1 A · g^{-1}. The specific capacitance of 56 F · g^{-1} still exists when the current density is increased to 100 A · g^{-1} [117]. Chen et al. used cellulose nanocrystals (CNC) to adjust the structure of GBFs. CNC nanorods can not only improve the serious accumulation of graphene sheets in GBFs but also inhibit the possible bending and folding of graphene sheets in the process of fiber-forming, so as to form ordered nanopore structure. The composite GBFs were assembled into a supercapacitor with a conductivity of 64.7 S · cm^{-1} and a specific capacitance of 208.2 F · cm^{-3}, which has excellent electrochemical performance [99]. In addition, they also use graphene hollow fiber prepared by the electrochemical method as the electrode of fiber-like supercapacitor [121], and the additional inner surface of hollow fiber can provide more contact area with electrolyte. Under the current density of 0.1 A · g^{-1}, the specific capacitance of the assembled solid-state supercapacitor can reach 178 F · g^{-1}, and it has good rate performance and cycle stability. Guoxing et al. prepared graphene/conductive polymer composite hollow fiber with the hydrothermal method. The combination of hollow structure and pseudocapacitance provided by conductive polymer greatly improved the capacity of the capacitor and provided a new idea for the improvement of supercapacitor capacitance [149].

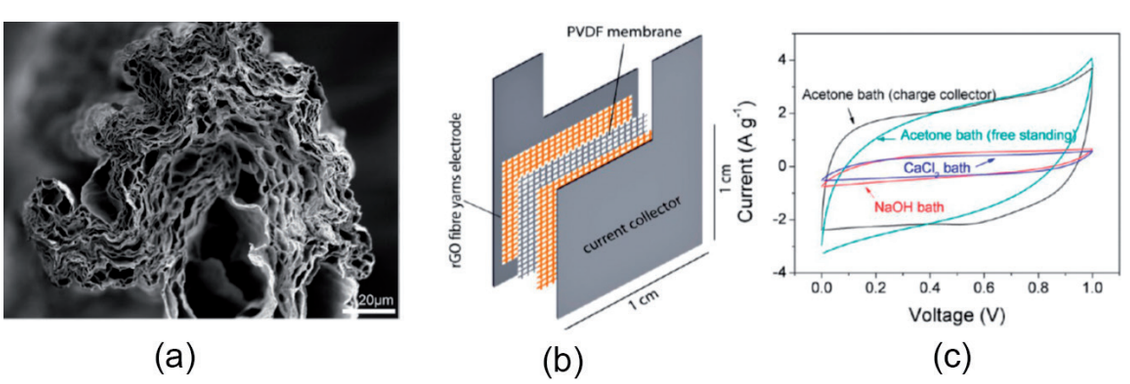

Figure 14.
Porous graphene fiber and its supercapacitor. (a) SEM image of porous fibers. (b) Schematic illustration of the structure of supercapacitor. (c) CV curves of graphene fibers prepared in different coagulation baths.

4.2.3 Energy conversion

4.2.3.1 Actuator

Actuators are a kind of stimuli-sensitive device that can respond to external stimuli, such as humidity, temperature, and electrical changes, and transfer the stimulus into deformation or motion [126, 127]. Due to quantum mechanics and electrostatic double-layer effect, graphene may cause space warping or plane expansion under the charge injection. In addition, the intercalation or removal of ions or molecules in graphene products under external stimulation will also lead to the bending, twisting, and even reversible change of the interlayer spacing. In this way, the type and degree of deformation can be controlled by the composition and surface chemical state of graphene [150, 151].

Jia et al. showed an electrochemical fiber driver with high driving activity and durability based on GF/polypyrrole (GF/PPY) double-layer structure, as shown in **Figure 15**. Because of the asymmetry of the structure, GF/PPY fiber shows reversible bending deformation under the condition on positive and negative charges. As shown in **Figure 15**, when a positive voltage is applied to GF/PPY fiber, graphene will shrink and expand due to anion discharged from PPY, and the fiber will bend to the left. When a negative voltage is applied, GF/PPY fiber can bend to the right [152].

Compared with rGO, GO has more oxygen functional groups, so it is more sensitive to water. Based on this principle, Huhu et al. fabricated an asymmetric rGO/GO fiber by region-selective laser reduction along the GO fiber. When exposed to humid air, the rGO/GO fiber can bend to the rGO side and then return to its original state after air moisture dispersion. After that, they made a twisted GO fiber by rotating the GO hydrogel fibers in the direction of rotation. The spiral geometry inside them was the main reason for the reversible rotation in the moist air.

4.2.3.2 Solar cell

Wearable solar cells can supply power to flexible smart devices at any time, while GBFs can be used as electrode materials to achieve this new function. Peng et al.

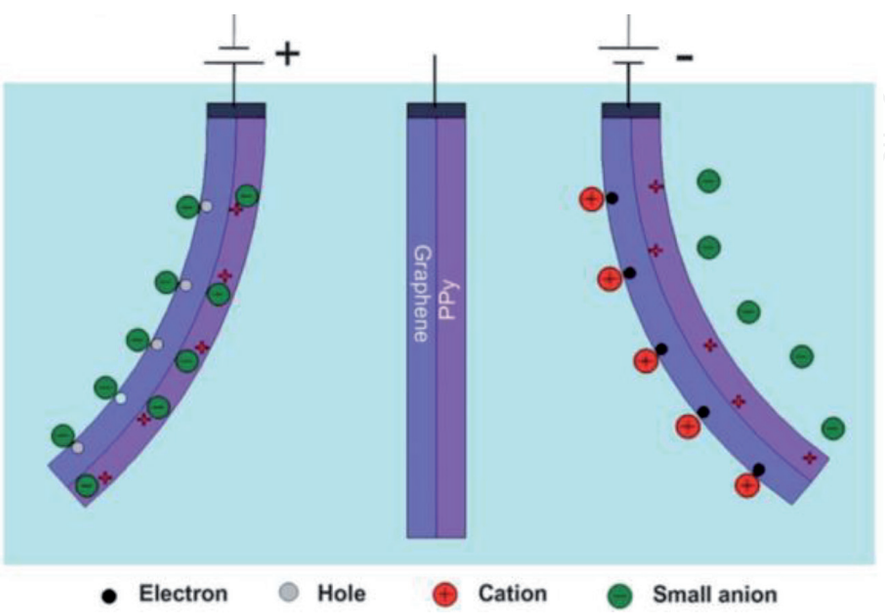

Figure 15.
Schematic illustration of the expansion-contraction mechanisms of the GF/PPY bilayer structure. Charges in each electrode are completely balanced by ions from the electrolyte.

obtained GBFs by wet spinning and then made its surface loaded with Pt metal particles by electrodeposition to the obtained counter electrode. The titanium wire with titanium dioxide microtubules on the surface is used as the working electrode; the dye-sensitized solar cell (DSSC) has an energy conversion efficiency of 8.45%, which is much higher than other linear photovoltaic devices. The continuous collection of energy can be realized by putting linear solar cells into conventional clothes [153]. The high surface properties and good electrical and electrochemical properties of graphene are the important reasons to improve the performance of fiber DSSC.

5. Conclusions and perspective

This chapter mainly summarizes the main preparation methods, properties, and application fields of CNT, CF, and GBF materials. Among them, CNTs have unique one-dimensional nanostructures and excellent mechanical, electrical, and optical properties. Through various methods of modification, researchers continue to prepare CNT composite nanomaterials with excellent performance, which has a good application prospect. Starting from the needs of the application field, it is the trend to study the carbon nanotube composite materials in the future to expect to obtain the high-efficiency structure which is corresponding to the application performance. Although some progress has been made in the preparation and properties of carbon nanotube composites, the mechanism of improving the properties of composites and the dispersion of carbon nanotubes still need to be explored.

CF is a new type of fiber material with high strength and high modulus, which contains more than 95% carbon. Its quality is lighter than that of aluminum, but its strength is higher than that of steel, and it has the characteristics of corrosion resistance and high-temperature resistance. It is an important material in the military industry and civil use. With the rapid development of CF composite and the continuous improvement of molding technology, its application scope is expanding day by day, and it shows good application potential in many fields. However, the physical and chemical properties of CF composites are complex, so it is necessary to study the basic theories of physical and chemical properties, mechanics, and heat, so as to improve the performance of CF composites.

GBFs have achieved great success in functional application, and it is far more amazing than CF. So far, various preparation methods have been studied and used in large-scale production of GBFs, which provides a positive impetus for the future application of GBFs. GBFs have been given new performance and function and provide new opportunities for various applications, including fiber-optic actuators, batteries, super electric containers, dye-sensitized solar cells, and sensors.

GBFs are a kind of graphene nanosheet assembled in one-dimensional space. At present, the structure of GBFs can be regulated in the following aspects: (1) Diameter. Generally, the diameter of GBFs is 10–100 μm. If it is prepared by electrospinning, its diameter can be controlled below 500 μm. (2) Porosity. On the one hand, it can be prepared by self-assembly, rolling, graphitization, and sintering; on the other hand, it can be prepared by freeze-drying, air spinning, and other methods. In addition, graphene hollow fiber can also be prepared. (3) Orientation. The arrangement of graphene sheets has a great influence on the properties of GBFs. The GBFs with a high degree of orientation can be obtained by the stress field orientation effect in the wet spinning process, the self-assembly in the electrochemical deposition process, and the second phase auxiliary orientation effect in the composite fiber. (4) Section morphology. It is difficult to maintain the circular cross section of the fiber, which is generally irregular. At present, the conventional method is to

adjust the fiber cross-sectional shape by adjusting the spinneret hole shape, but the research progress is slow.

In order to meet the needs of different applications, graphene composite fibers appear. The additive materials include metal, inorganic, and polymer materials, such as silver nanowires, silicon nanoparticles, molybdenum disulfide nanoparticles, polypyrrole nanoparticles, etc. Basically, any nanomaterial can be added to GBFs to get graphene composite fiber. But one of the key problems is to control the structure of the composite fiber. The main control factor is the morphology of the second phase and its distribution in the fiber. For GBFs and its composite fiber, the main problems are as follows: (1) Compared with the graphene nanoflakes, the properties of GBFs are greatly cracked. (2) GBFs are composed of layers, which are very different from the chain structure of the traditional chemical fiber, so its flexibility is poor. (3) It is difficult to realize continuous production. Even with the most suitable wet spinning method for continuous production, its continuous production is very difficult, and the yield is very low.

Although GBFs are faced with many problems, remarkable achievements have been made. Compared with CF, GBFs have the characteristics of high strength, high modulus, conductivity, and certain flexibility, which have developed into a new type of high-performance fiber. On the other hand, graphene composite fiber is committed to develop into a new type of multifunctional intelligent fiber. This kind of fiber starts from modifying the traditional general-purpose fiber to improve some aspects of the performance of the general-purpose fiber and to develop new kinds of fiber, such as graphene/nano titanium oxide composite fiber. It can also develop new fiber performance and functions, such as energy storage, and finally realize multiple functions such as perception, judgment, correspondence, information transmission, etc. on the fiber and become a new type of intelligent material. Therefore, GBFs and its composite fiber will be widely used in aerospace, energy sensing, intelligent life, and other fields in the future.

Acknowledgements

The authors thank the support of Stevens startup fund.

Conflict of interest

The authors declare no conflict of interest.

IntechOpen

Author details

Yan Xu and Xian Zhang*
Stevens Institute of Technology, Hoboken, NJ, Untied States

*Address all correspondence to: xian.zhang@stevens.edu

IntechOpen

References

[1] Zhang X. Characterization of layer number of two-dimensional transition metal diselenide semiconducting devices using Si-peak analysis. Advances in Materials Science and Engineering. 2019;**2019**:7865698

[2] Li Y, Ye F, Xu J, Zhang W, Feng P, Zhang X. Gate-tuned temperature in a hexagonal boron nitride-encapsulated 2D semiconductor devices. IEEE Transactions on Electronic Devices. 2018;**65**(10):4068-4072

[3] Li Y, Chernikov A, Zhang X, Rigosi A, Hill HM, van der Zande AM, et al. Measurement of the optical dielectric function of monolayer transition-metal dichalcogenides: MoS_2, $MoSe_2$, WS_2, WSe_2. Physical Review B. 2014;**90**(20):205422

[4] Zhang X, Sun D, Li Y, Lee G-H, Cui X, Chenet D, et al. Measurement of lateral and interfacial thermal conductivity of single- and bilayer MoS_2 and $MoSe_2$ using optothermal Raman technique. ACS Applied Materials & Interfaces. 2015;**7**(46):25923-25929

[5] Zhang X, Chenet D, Kim B, Yu J, Tang J, Nuckolls C, et al. Fabrication of hundreds of field effect transistors on a single carbon nanotube for basic studies and molecular devices. Journal of Vacuum Science and Technology B. 2013;**31**(6):06FI01

[6] Yin D, Dun C, Gao X, Liu Y, Zhang X, Carroll D, et al. Controllable colloidal synthesis of Tin(II) chalcogenide nanocrystals and their solution-processed flexible thermoelectric thin films. Small. 2018;**14**(33):1801949

[7] Wu S, Wang L, Lai Y, Shan W-Y, Aivazian G, Zhang X, et al. Multiple hot-carrier collection in photo-excited graphene Moiré superlattices. Science Advances. 2016;**2**(5):e1600002

[8] De Vellis A, Gritsenko D, Lin Y, Wu Z, Zhang X, Pan Y, et al. Drastic sensing enhancement using acoustic bubbles for surface-based microfluidic sensors. Sensors and Actuators B: Chemical. 2017;**243**:298-302

[9] Gogotsi Y, Presser V. Carbon Nanomaterials. Florida, United States: CRC Press; 2013

[10] De Volder MF, Tawfick SH, Baughman RH, Hart AJ. Carbon nanotubes: Present and future commercial applications. Science. 2013;**339**(6119):535-539. DOI: 10.1126/science.1222453

[11] Gojny F, Wichmann M, Köpke U, Fiedler B, Schulte K. Carbon nanotube-reinforced epoxy-composites: Enhanced stiffness and fracture toughness at low nanotube content. Composites Science and Technology. 2014;**64**(15):2363-2371. DOI: 10.1016/j.compscitech.2004.04.002

[12] Hiremath N, Mays J, Bhat G. Recent developments in carbon fibers and carbon nanotube-based fibers: A review. Polymer Reviews. 2017;**57**(2):339-368. DOI: 10.1080/15583724.2016.1169546

[13] Gong K, Pan Z, Korayem AH, Qiu L, Li D, Collins F, et al. Reinforcing effects of graphene oxide on portland cement paste. Journal of Materials in Civil Engineering. 2014;**27**(2):A4014010. DOI: 10.1061/(ASCE)MT.1943-5533.0001125

[14] Lu C, Lu Z, Li Z, Leung CK. Effect of graphene oxide on the mechanical behavior of strain hardening cementitious composites. Construction and Building Materials. 2016;**120**:457-464. DOI: 10.1016/j.conbuildmat.2016.05.122

[15] Zhu Y, Murali S, Cai W, Li X, Suk JW, Potts JR, et al. Graphene and

graphene oxide: Synthesis, properties, and applications. Advanced Materials. 2010;**22**(35):3906-3924. DOI: 10.1002/adma.201001068

[16] Chatterjee S, Nüesch F, Chu BT. Comparing carbon nanotubes and graphene nanoplatelets as reinforcements in polyamide 12 composites. Nanotechnology. 2011;**22**(27):275714. DOI: 10.1088/0957-4484/22/27/275714

[17] Lingqi C, Xiaowei Y, Xiaomeng F, Meng C, Xiaokang M, Laifei C, et al. Mechanical and electromagnetic shielding properties of carbon fiber reinforced silicon carbide matrix composites. Carbon. 2015;**95**:10-19. DOI: 10.1016/j.carbon.2015.08.011

[18] Rezaei F, Ynus R, Ibrahim NA. Effect of fiber length on thermomechanical properties of short carbon fiber reinforced polypropylene composites. Materials & Design. 2009;**30**(2):260-263. DOI: 10.1016/j.matdes.2008.05.005

[19] Waseem K, Rahul S, Parveen S. Carbon nanotube-based polymer composites: Synthesis, properties and applications. Carbon Nanotubes. 2016. DOI: 10.5772/62497

[20] Weng WZ, He SS, Song HY, Li XQ, Cao LH, Hu YJ, et al. Aligned carbon nanotubes reduce hypertrophic scar via regulating cell behavior. ACS Nano. 2018;**12**:7601-7612. DOI: 10.1021/acsnano.7b07439

[21] He SS, Zhang YY, Qiu LB, Zhang LS, Xie Y, Pan J, et al. Chemical-to-electricity carbon: Water device. Advanced Materials. 2018;**30**(18):1707635. DOI: 10.1002/adma.201707635

[22] Thostenson ET, Li WZ, Wang DZ. Carbon nano-tube/carbon fiber hybrid multiscale composites. Journal of Applied Physics. 2002;**91**(9):6034-6037. DOI: 10.1063/1.1466880

[23] Davis VA, Parra-Vasquez ANG, Green MJ, Rai PK, Behabtu N, Prieto V, et al. True solutions of single-walled carbon nanotubes for assembly into macroscopic materials. Nature nanotechnology. 2009;**4**:830-834. DOI: 10.1038/NNANO.2009.302

[24] Evans WJ, Hu L, Keblinski P. Thermal conductivity of graphene ribbons from equilibrium molecular dynamics: Effect of ribbon width, edge roughness, and hydrogen termination. Applied Physics Letters. 2010;**96**:203112. DOI: 10.1063/1.3435465

[25] Dalton AB, Collins S, Munoz E, Razal JM, Ebron VH, Ferraris JP, et al. Super-tough carbon-nanotube fibres-these extraordinary composite fibres can be woven into electronic textiles. Nature. 2003;**423**:703-703. DOI: 10.1039/B312092A

[26] Muhammad M, Ali R, Javed I. Production of carbon nanotubes by different routes-a review. Scientific Research. 2011;**1**:29-34. DOI: 10.4236/jeas.2011.11004

[27] Bin W, Yanfeng M, Yingpeng W, Na L, Yi H, Yongsheng C. Direct and large scale electric arc discharge synthesis of boron and nitrogen doped single-walled carbon nanotubes and their electronic properties. Carbon. 2009;**47**(8):2112-2115. DOI: 10.1016/j.carbon.2009.02.027

[28] Naiqin Z, Chunnian H, Zhaoyang J, Jiajun L, Yongdan L. Fabrication and growth mechanism of carbon nanotubes by catalytic chemical vapor deposition. Materials Letters. 2006;**60**(2):159-163. DOI: 10.1016/j.matlet.2005.08.009

[29] Qingwen L, Hao Y, Jin Z, Zhongfan L. Effect of hydrocarbons precursors on the formation of carbon nanotubes in chemical vapor deposition. Carbon. 2004;**42**(4):829-835. DOI: 10.1016/j.carbon.2004.01.070

[30] Yibo Y, Jianwei M, Zhihong Y, Fangxing X, Hongbin Y, Yanhui Y. Carbon nanotube catalysts: Recent advances in synthesis, characterization and applications. Chemical Society Reviews. 2015;**44**(10):3295-3346. DOI: 10.1039/c4cs00492b

[31] Andrea S, Caterina P, Anita C, Girolamo G, Danilo V, Janos BN. Synthesis methods of carbon nanotubes and related materials. Materials. 2010;**3**(5):3092-3140. DOI: 10.3390/ma3053092

[32] Somu C, Karthi A, Sanjay S, Karthikeyan R, Dinesh S, Ganesh N. Synthesis of various forms of carbon nanotubes by arc discharge methods—Comprehensive review. International Research Journal of Engineering and Technology. 2017;**4**(1):344-354

[33] Kerdcharoen T, Wongchoosuk C. Carbon nanotube and metal oxide hybrid materials for gas sensing. Semiconductor Gas Sensors, DOI. 2013:386-407. DOI: 10.1533/9780857098665.3.386

[34] Deepalekshmi P, Kishor KS, Yves G, Qipeng G, Sabu T. Carbon nanotube based elastomer composites—An approach towards multifunctional materials. Journal of Materials Chemistry C. 2014;**40**(2):8446-8485. DOI: 10.1039/C4TC01037J

[35] Li YL, Kinloch IA, Windle AH. Direct spinning of carbon nanotube fibers from chemical vapor deposition synthesis. Science. 2004;**304**(5668):276-278. DOI: 10.1126/science.1094982

[36] Mubarak NM, Abdullah EC, Jayakumar NS, Sahu JN. An overview on methods for the production of carbon nanotubes. Journal of Industrial and Engineering Chemistry. 2014;**20**(4):1186-1197. DOI: 10.1016/j.jiec.2013.09.001

[37] Muhammad OM, Sylvain H, Khalid L. Carbon nanofiber based buckypaper used as a thermal interface material. Carbon. 2011;**49**(12):3820-3828. DOI: 10.1016/j.carbon.2011.05.015

[38] Demczyk BG, Wang YM, Cumings J, Hetman M, Han W, Zettl A, et al. Direct mechanical measurement of the tensile strength and elastic modulus of multiwalled carbon nanotubes. Materials Science and Engineering: A. 2002;**334**(1-2):173-178. DOI: 10.1016/S0921-5093(01)01807-X

[39] Coleman JN, Khan U, Gunko YK. Mechanical reinforcement of polymers using carbon nanotubes. Advanced Materials. 2006;**18**(6):689-706. DOI: 10.1002/adma.200501851

[40] Dresselhaus MS, Dresselhaus G, Charlier JC, Hernandez E. Electronic, thermal and mechanical properties of carbon nanotubes. The Royal Society. 2004;**362**(1823):2065-2098. DOI: 10.1098/rsta.2004.1430

[41] Florian HG, Malte HG, Wichmann BF, Karl S. Influence of different carbon nanotubes on the mechanical properties of epoxy matrix composites—A comparative study. Composites Science and Technology. 2005;**65**(15-16):2300-2313. DOI: 10.1016/j.compscitech.2005.04.021

[42] Aliev AE, Lima MH, Silverman EM, Baughman RH. Thermal conductivity of multi-walled carbon nanotube sheets: Radiation losses and quenching of phonon modes. Nanotechnology. 2009;**21**(3):035709. DOI: 10.1088/0957-4484/21/3/035709

[43] Lindsay L, Broido DA, Natalio M. Diameter dependence of carbon nanotube thermal conductivity and extension to the graphene limit. Physical Review B. 2010;**82**:161402. DOI: 10.1103/PhysRevB.82.161402

[44] Hone J, Batlogg B, Benes Z, Johnson AT, Fischer JE. Quantized phonon spectrum of single-wall

carbon nanotubes. Science. 2000;**289**(5485):1730-1733. DOI: 10.1126/science.289.5485.1730

[45] Wei F, Mengmeng Q, Yiyu F. Toward highly thermally conductive all-carbon composites: Structure control. Carbon. 2016;**109**:575-597. DOI: 10.1016/j.carbon.2016.08.059

[46] Chang L, Huiming C. Carbon nanotubes: Controlled growth and application. Materials Today. 2013;**16**(1-2):19-28. DOI: 10.1016/j.mattod.2013.01.019

[47] Key HA, Won SK, Yong SP, Jeongmi M, Dong JB. Electrochemical properties of high-power super-capacitors using single-walled carbon nanotube electrodes. Advanced Functional Materials. 2001;**11**(5):387-391. DOI: 10.1002/1616-3028(200110)11:5<387::AID-ADFM387>3.0.CO;2-G

[48] Bin X, Feng W, Fang W, Shi C, Gaoping C, Yusheng Y. Single-walled carbon nanotubes as electrode materials for supercapacitors. Chinese Journal of Chemistry. 2006;**24**(11):1505-1508. DOI: 10.1002/cjoc.200690284

[49] Chichang H, Jenhong S, Tenchin W. Modification of multi-walled carbon nanotubes for electric double-layer capacitors: Tube opening and surface functionalization. Journal of Physics and Chemistry of Solids. 2007;**68**(12):2353-2362. DOI: 10.1016/j.jpcs.2007.07.002

[50] Minjung J, Euigyung J, Youngseak L. The surface chemical properties of multi-walled carbon nanotubes modified by thermal fluorination for electric double-layer capacitor. Applied Surface Science. 2015;**347**:250-257. DOI: 10.1016/j.apsusc.2015.04.038

[51] Guoping W, Lei Z, Jiujun Z. A review of electrode materials for electrochemical supercapacitors. Chemical Society Reviews. 2012;**41**(2):797-828. DOI: 10.1039/c1cs15060j

[52] Frank E, Steudle LM, Ingildeev D, Spörl JM, Buchmeiser MR. Carbon fibers: Precursor systems, processing, structure, and properties. Angewandte Chemie International Edition. 2014;**53**(21):5262-5298. DOI: 10.1002/anie.201306129

[53] Yun Z, Zhaojun L, Huiqi W, Jingli S, Jincai Z. Microstructure and thermal/mechanical properties of short carbon fiber-reinforced natural graphite flake composites with mesophase pitch as the binder. Carbon. 2013;**53**:313-320. DOI: 10.1016/j.carbon.2012.11.013

[54] He F. Carbon Fiber and Application Technology. Shanghai, China: Chemical Industry Press; 2004

[55] Soutis C. Carbon fiber reinforced plastics in aircraft construction. Materials Science and Engineering: A. 2005;**412**(1-2):171-176. DOI: 10.1016/j.msea.2005.08.064

[56] Krenkel W. Carbon fiber reinforced CMC for high-performance structures. International Journal of Applied Ceramic Technology. 2004;**1**(2):188-200. DOI: 10.1111/j.1744-7402.2004.tb00169.x

[57] Erik F, Frank H, Michael RB. Carbon fibers: Precursors, manufacturing, and properties. Macromolecular Materials and Engineering. 2012;**297**(6):493-501. DOI: 10.1002/mame.201100406

[58] Zhaokun M, Jingli S, Yan S. Carbon with high thermal conductivity, prepared from ribbon-shaped mesosphase pitch-based fibers. Carbon. 2006;**44**(7):1298-1301. DOI: 10.1016/j.carbon.2006.01.015

[59] Van Hattum FW, Bernardo CA, Finegan JC, Tibbetts GG, Alig RL,

Lake ML. A study of the thermo-mechanical properties of carbon fiber-polypropylene composites. Polymer Composites. 2004;**20**(5):683-688. DOI: 10.1002/pc.10391

[60] Basu S, Bhattacharyya P. Recent developments on graphene and graphene oxide based solid state gas sensors. Sensors and Actuators B: Chemical. 2012;**173**:1-21. DOI: 10.1016/j.snb.2012.07.092

[61] Noveselov KS, Geim AK, Morozov SV, Jiang D, Zhang Y. Electric field effect in atomically thin carbon films. Science. 2004;**306**(5696):666-669. DOI: 10.1126/science.1102896

[62] Wongbong C, Indranil L, Raghunandan S, Yong SK. Synthesis of Graphene and its applications: A review. Critical Reviews in Solid State and Materials Sciences. 2010;**35**:1. DOI: 10.1080/10408430903505036

[63] Fancheng M, Weibang L, Qingwen L, Joonhyung B, Youngseok O, Tsuwei C. Graphene-based fibers: A review. Advanced Materials. 2015;**27**:5113-5131. DOI: 10.1002/adma.201501126

[64] Alexander AB, Suchismita G, Wenzhong B, Irene C. Superior thermal conductivity of single-layer graphene. Nano Letters. 2008;**8**(3):902-907. DOI: 10.1021/nl0731872

[65] Lee CG, Wei XD, Kysar JW, Hong J. Measurement of the elastic properties and intrinsic strength of monolayer graphene. Science. 2008;**321**(5887):385-388. DOI: 10.1126/science.1157996

[66] Novoselov KS, Geim AK, Morozov SV, Jiang D, Katsnelson MI, Grigorieva IV, et al. Two-dimensional gas of massless dirac fermions in graphene. Nature. 2005;**438**:197-200

[67] Zhang YB, Tan YW, Stormer HL, Kim P. Experimental observation of the quantum Hall effect and Berry's phase in graphene. Nature. 2005;**438**:201-204

[68] Bolotin KI, Sikes KJ, Jiang Z, Klima M, Fudenberg G, Hone J, et al. Ultrahigh electron mobility in suspended graphene. Solid State Communications. 2008;**146**:351-355. DOI: 10.1016/j.ssc.2008.02.024

[69] Morozov SV, Novoselov KS, Katsnelson MI, Schedin F, Elias DC, Jaszczak JA, et al. Giant intrinsic carrier mobilities in graphene and its bilayer. Physical Review Letters. 2008;**100**:016602. DOI: 10.1103/PhysRevLett.100.016602

[70] Chen HJ, Jang C, Xiao SD, Ishigami M, Fuhrer MS. Intrinsic and extrinsic performance limits of graphene devices on SiO_2. Nature Nanotechnology. 2008;**3**:206-209. DOI: 10.1038/nnano.2008.58

[71] Si YC, Samulski ET. Synthesis of water soluble graphene. International Nano Letters. 2008;**8**:1679-1682. DOI: 10.1021/nl080604h

[72] Pei S, Zhao J, Du J, Ren W, Cheng HM. Direct reduction of graphene oxide films into highly conductive and flexible graphene films by hydrohalic acids. Carbon. 2010;**48**:4466-4474. DOI: 10.1016/j.carbon.2010.08.006

[73] Moon K, Lee J, Ruoff RS, Lee H. Reduced graphene oxide by chemical graphitization. Nature Communications. 2010;**1**:73-78. DOI: 10.1038/ncomms1067

[74] Becerril HA, Mao J, Liu Z, Stoltenberg RM, Bao Z, Chen YS. Evaluation of solution-processed reduced graphene oxide films as transparent conductors. ACS Nano. 2008;**2**:463-470. DOI: 10.1021/nn700375n

[75] McAllister MJ, Li J, Adamson DH, Schniepp HC, Abdala AA, Liu J, et al.

Single sheet functionalized graphene by oxidation and thermal expansion of graphite. Chemistry of Materials. 2007;**19**:4396-4404. DOI: 10.1021/cm0630800

[76] Zhu YW, Stoller MD, Cai WW, Velamakanni A, Piner RD, Chen D, et al. Exfoliation of graphite oxide in propylene carbonate and thermal reduction of the resulting graphene oxide platelets. ACS Nano. 2010;**4**:1227-1233. DOI: 10.1021/nn901689k

[77] Wang ZJ, Zhou XZ, Zhang J, Boey F, Zhang H. Direct electrochemical reduction of single-layer graphene oxide and subsequent functionalization with glucose oxidase. The Journal of Chemical Physics. 2009;**113**:14071-14075. DOI: 10.1021/jp906348x

[78] Haiyun S, Zhen X, Chao G. Multifunctional, ultra-flyweight. Synergistically Assembled Carbon Aerogels. Advanced Materials. 2013;**25**(18):2554. DOI: 10.1002/adma.201204576

[79] Stefania N, Daniel C, Luisa F, Maria CG, Francisco DM. Three dimensional macroporous architectures and aerogels built of carbon nanotubes and/or graphene: Synthesis and applications. Chemical Society Reviews. 2013;**43**(2):794-830. DOI: 10.1039/C2CS35353A

[80] Juergen B, Michael S, Matthew S, Marcus AW, Monika MB, Klint AR, et al. Advanced carbon aerogels for energy applications. Energy & Environmental Science. 2011;**4**:656-667. DOI: 10.1039/C0EE00627K

[81] Zakharchenko KV, Annalisa F, Los JH, Katsnelson MI. Melting of graphene: From two to one dimension. Journal of Physics: Condensed Matter. 2011;**23**(20):202202. DOI: 10.1088/0953-8984/23/20/202202

[82] Seong GK, David T. Melting the fullerenes: A molecular dynamics study. Physical Review Letters. 1994;**72**(15):2418. DOI: 10.1103/PhysRevLett.72.2418

[83] Liu YJ, Liang H, Xu Z, Xi JB, Chen GF, Gao WW, et al. Superconducting continuous graphene fibers via calcium intercalation. ACS Nano. 2017;**11**:4301-4306. DOI: 10.1021/acsnano.7b01491

[84] Meng J, Nie WQ, Zhang K, Xu FJ, Ding X, Wang SR, et al. Enhancing electrochemical performance of graphene fiber-based supercapacitors by plasma treatment. ACS Applied Materials & Interfaces. 2018;**10**:13652-13659. DOI: 10.1021/acsami.8b04438

[85] Choi SJ, Yu HY, Jang JS, Kim MH, Kim SJ, Jeong HS, et al. Nitrogen-doped single graphene fiber with platinum water dissociation catalyst for wearable humidity sensor. Small. 2018;**14**:1703934. DOI: 10.1002/smll.201703934

[86] Zhen X, Chao G. Graphene chiral liquid crystals and macroscopic assembled fibres. Nature Communications. 2011;**2**:571. DOI: 10.1038/ncomms1583

[87] Zhen X, Haiyan S, Xiaoli Z, Chao G. Ultrastrong fibers assembled from giant graphene oxide sheets. Advanced Materials. 2012;**25**(2):188. DOI: 10.1002/adma.201203448

[88] Xiang C, Young CC, Wang X, Yan Z, Hwang CC, Cerioti G. Large flake graphene oxide fibers with unconventional 100% knot efficiency and highly aligned small flake graphene oxide fibers. Advanced Materials. 2013;**25**(33):4592-4597. DOI: 10.1002/adma.201301065

[89] Zhen X, Yingjun L, Xiaoli Z, Li P, Haiyan S, Yang X, et al. Ultrastiff and strong graphene fibers via full-scale synergetic defect engineering. Advanced Materials. 2016;**28**(30):6449-6456. DOI: 10.1002/adma.201506426

[90] Yingjun L, Zhen X, Jianmig Z, Peigang L, Chao G. Superb electrically conductive graphene fibers via doping strategy. Advanced Materials. 2016;**28**(36):7941-7947. DOI: 10.1002/adma.201602444

[91] Shaohua C, Wujun M, Yanhua C, Zhe W, Bin S, Lu W, et al. Scalable non-liquid-crystal spinning of locally aligned graphene fibers for high-performance wearable supercapacitors. Nano Energy. 2015;**15**:642-653. DOI: 10.1016/j.nanoen.2015.05.004

[92] Xiaoteng D, Jie B, Tong X, Changxia L, Huimin Z, Liangti Q. A novel nitrogen-doped graphene fiber microelectrode with ultrahigh sensitivity for the detection of dopamine. Electrochemistry Communications. 2016;**72**:122-125. DOI: 10.1016/j.elecom.2016.09.021

[93] Xiaoteng D, Yang Z, Chuangang H, Yue H, Zelin D, Nan C, et al. Spinning fabrication of graphene/polypyrrole composite fibers for all-solid-state, flexible fibriform supercapacitors. Journal of Materials Chemistry A. 2014;**2**(31):12355-12360. DOI: 10.1039/C4TA01230E

[94] Wujun M, Shaohua C, Shengyuan Y, Wenping C, Wei W, Yanhua C. Flexible all-solid-state asymmetric supercapacitor based on transition metal oxide nanorods/reduced graphene oxide hybrid fibers with high energy density. Carbon. 2017;**133**:151-158. DOI: 10.1016/j.carbon.2016.11.051

[95] Wujun M, Shaohua C, Shengyuan Y, Meifang Z. Hierarchically porous carbon black/graphene hybrid fibers for high performance flexible supercapacitors. RSC Advances. 2016;**6**(55):50112-50118. DOI: 10.1039/C6RA08799J

[96] Wujun M, Shaohua C, Shengyuan Y, Wenping C, Wei W, Meifang Z. Bottom-up fabrication of activated carbon fiber for all-solid-state supercapacitor with excellent electrochemical performance. ACS Applied Materials & Interfaces. 2016;**8**(23):14622-14627. DOI: 10.1021/acsami.6b04026

[97] Wujun M, Shaohua C, Shengyuan Y, Wenping C, Yanhua C, Yiwei G, et al. Hierarchical MnO_2 nanowire/graphene hybrid fibers with excellent electrochemical performance for flexible solid-state supercapacitors. Journal of Power Sources. 2016;**306**(29):481-488. DOI: 10.1016/j.jpowsour.2015.12.063

[98] Shaohua C, Wujun M, Hengxue X, Yanhua C, Shengyuan Y, Wei W, et al. Conductive, tough, hydrophilic poly(vinyl alcohol)/graphene hybrid fibers for wearable supercapacitors. Journal of Power Sources. 2016;**319**(1):271-280. DOI: 10.1016/j.jpowsour.2016.04.030

[99] Guoyin C, Tao C, Kai H, Wujun M, Mike T, Yanhua C, et al. Robust, hydrophilic graphene/cellulose nanocrystal fiber-based electrode with high capacitive performance and conductivity. Carbon. 2018;**127**:218-227. DOI: 10.1016/j.carbon.2017.11.012

[100] Mochen L, Xiaohong Z, Xiang W, Yue R, Jinliang Q. Ultrastrong graphene-based fibers with increased elongation. Nano Letters. 2016;**16**(10):6511-6515. DOI: 10.1021/acs.nanolett.6b03108

[101] Yang Z, Changcheng J, Chuangang H, Zhlin D, Jiangli X, Yuning M, et al. Large-scale spinning assembly of neat, morphology-defined, graphene based hollow fibers. ACS Nano. 2013;**7**(3):2406-2412. DOI: 10.1021/nn305674a

[102] Dan L, Marc BM, Scott G, Richard BK, Gordon GW. Processable aqueous dispersions of graphene nanosheets. Nature Nanotechnology. 2008;**3**(2):101-105. DOI: 10.1038/nnano.2007.451

[103] Xiang C, Behabtu N, Lin Y, Chae HG, Young CC, Genorio B, et al. Graphene nanoribbons as an advanced precursor for making carbon fiber. ACS Nano. 2013;**7**(2):1628-1637. DOI: 10.1021/nn305506s

[104] Jang EY, Kim WJ, Kim T, Kang TJ, Kim YH, Carretero GJ, et al. Fibers of reduced graphene oxide nanoribbons. Nanotechnology. 2012;**23**(23):235601. DOI: 10.1088/0957-4484/23/23/235601

[105] Dong Z, Jiang C, Cheng H, Zhao Y, Shi G, Jiang L, et al. Facile fabrication of light, flexible and multifunctional graphene fibers. Advanced Materials. 2012;**24**(10):1856-1861. DOI: 10.1002/adma.201200170

[106] Yu D, Goh K, Wang H, Wei L, Jiang W, Zhang Q, et al. Scalable synthesis of hierarchically structured carbon nanotube-graphene fibres for capacitive energy storage. Nature Nanotechnology. 2014;**9**(7):555-562. DOI: 10.1038/nnano.2014.93

[107] Qishi T, Zhen X, Yingjun L, Bo F, Li P, Jiabin X, et al. Dry spinning approach to continuous graphene fibers with high toughness. Nanoscale. 2017;**9**(34):12335-12342. DOI: 10.1039/C7NR03895J

[108] Muge A, Geunsik L, Cecilia M, Adam P, Robert MW, Manish C, et al. The role of oxygen during thermal reduction of graphene oxide studied by infrared absorption spectroscopy. The Journal of Physical Chemistry C. 2011;**115**(40):19761-19781. DOI: 10.1021/jp2052618

[109] Hae-kyung J, Yun PL, Mei HJ, Eun SK, Jung JB, Young HL. Thermal stability of graphite oxide. Chemical Physics Letters. 2009;**470**(4-6):255-258. DOI: 10.1016/j.cplett.2009.01.050

[110] Qing C, Yuning M, Chuangang H, Yang Z, Huibo S, Nan C, et al. MnO_2-modified hierarchical graphene fiber electrochemical supercapacitor. Journal of Power Sources. 2014;**247**:32-39. DOI: 10.1016/j.jpowsour.2013.08.045

[111] Jihao L, Jingye L, Linfan L, Ming Y, Hongjuan M, Bowu Z. Flexible graphene fibers prepared by chemical reduction-induced self-assembly. Journal of Materials Chemistry A. 2014;**2**(18):6359-6362. DOI: 10.1039/C4TA00431K

[112] Chuangang H, Yang Z, Huhu C, Yanhong W, Zelin D, Changcheng J, et al. Graphene microtubings: controlled fabrication and site-specific functionalization. Nano Letters. 2012;**12**(11):5879-5884. DOI: 10.1021/nl303243h

[113] Jing F, Zelin D, Meiling Q, Ruonong F, Liangti Q. Monolithic graphene fibers for solid-phase microextraction. Journal of Chromatography A. 2013;**1320**:27-32. DOI: 10.1016/j.chroma.2013.10.065

[114] Xiaosong H. Fabrication and properties of carbon fibers. Materials. 2009;**2**(4):2369-2403. DOI: 10.3390/ma2042369

[115] Shayan S, Mark SR, Andrew IM, Joselito MR. Towards the knittability of graphene oxide fibres. Scientific Reports. 2015;**5**:14946. DOI: 10.1038/srep14946

[116] Xinming L, Tianshuo Z, Kunlin W, Ying Y, Jinquan W, Feiyu K, et al. Directly drawing self-assembled, porous, and monolithic graphene fiber from chemical vapor deposition grown graphene film and its electrochemical properties. Langmuir. 2011;**27**(19):12164-12171. DOI: 10.1021/la202380g

[117] Seyed HA, Rouhollah J, Dorna E, Maryam S, Zahra G, Sima AY, et al. High-performance multifunctional graphene yarns: Toward wearable all-carbon energy storage textiles.

ACS Nano. 2014;**8**(3):2456-2466. DOI: 10.1021/nn406026z

[118] Jiali Y, Mei W, Ping X, Seung HC, Jonghwan S, Ke G, et al. Ultrahigh-rate wire-shaped supercapacitor based on graphene fiber. Carbon. 2017;**119**:332-338. DOI: 10.1016/j.carbon.2017.04.052

[119] Yunming J, Mei Z, Hongwei L, Jianming W, Fanglan G. Controllable synthesis and electrochemical performance of hierarchically structured graphene fibers. Materials Chemistry and Physics. 2017;**193**:35-41. DOI: 10.1016/j.matchemphys.2017.02.014

[120] Lizhi S, Tong W, Yuan L, Lili J, Liangti Q, Zhuangjun F. Ultra-high toughness all graphene fibers derived from synergetic effect of interconnected graphene ribbons and graphene sheets. Carbon. 2017;**120**:17-22. DOI: 10.1016/j.carbon.2017.05.033

[121] Junjie Y, Wei W, Yang Z, Xiaowen D, Yunxia L, Lijun Y, et al. Highly flexible and shape-persistent graphene microtube and its application in supercapacitor. Carbon. 2018;**126**:419-425. DOI: 10.1016/j.carbon.2017.10.045

[122] Lianlian C, Yu L, Yang Z, Nan C, Liangti Q. Graphene-based fibers for supercapacitor applications. Nanotechnology. 2015;**27**(3):032001. DOI: 10.1088/0957-4484/27/3/032001

[123] Fei Z, Yang Z, Huhu C, Liangti Q. A graphene fibriform responsor for sensing heat, humidity, and mechanical changes. Angewandte Chemie International Edition. 2015;**54**(49):14951-14955. DOI: 10.1002/anie.201508300

[124] Yanhong W, Ke B, Chuangang H, Zhipan Z, Nan C, Huimin Z, et al. Flexible and wearable graphene/polypyrrole fibers towards multi-functional actuator applications. Electrochemistry Communications. 2013;**35**:49-52. DOI: 10.1016/j.elecom.2013.07.044

[125] Chunfei H, Yuanyuan S, Xiying L, Xiaoyang H, Ying W, Xinchang W, et al. Helical graphene oxide fibers as a stretchable sensor and an electrocapillary sucker. Nanoscale. 2016;**8**(20):10659-10668. DOI: 10.1039/C6NR02111E

[126] Huhu C, Jia L, Yang Z, Chuangang H, Zhipan Z, Nan C, et al. Graphene fibers with predetermined deformation as moisture-triggered actuators and robots. Angewandte Chemie International Edition. 2013;**52**(40):10482-10486. DOI: 10.1002/anie.201304358

[127] Huhu C, Yue H, Fei Z, Zelin D, Yanhong W, Nan C, et al. Moisture-activated torsional graphene-fiber motor. Advanced Materials;**26**(18):2909-2913. DOI: 10.1002/adma.201305708

[128] Fei L, Shuyan S, Dongfeng X, Hongjie Z. Folded structured graphene paper for high performance electrode materials. Advanced Materials. 2012;**24**(8):1089-1094. DOI: 10.1002/adma.201104691

[129] Wei A, Zhimin L, Jian J, Jianhui Z, Zhuzhu D, Zhanxi F, et al. Nitrogen and sulfur codoped graphene: Multifunctional electrode materials for high-performance li-ion batteries and oxygen reduction reaction. Advanced Materials. 2014;**26**(35):6186-6192. DOI: 10.1002/adma.201401427

[130] Jong GL, Youbin K, Ji YJ, Sungho C, Yongku K, Woong RY, et al. Fiber electrode by one-pot wet-spinning of graphene and manganese oxide nanowires for wearable lithium-ion batteries. Journal of Applied Electrochemistry. 2017;**47**(8):865-875. DOI: 10.1007/s10800-017-1085-y

[131] Minsu G, Seunghee K, Seungmin Y, Eunhee L, Sa HM, Soojin P, et al. Double locked silver-coated silicon nanoparticle/graphene core/shell fiber for high-performance lithium-ion battery anodes. Journal of Power Sources. 2015;**300**:351-357. DOI: 10.1016/j.jpowsour.2015.09.083

[132] Tatsumasa H, Yuanchuan Z, Junyu H, Zhiqiang W, Qingwen L, Zhigang Z, et al. Flexible lithium-ion fiber battery by the regular stacking of two-dimensional titanium oxide nanosheets hybridized with reduced graphene oxide. Nano Letters. 2017;**17**(6):3543-3549. DOI: 10.1021/acs.nanolett.7b00623

[133] Woon GC, Jian QH, Zheng LX, Xiangyin Q, Xiangyu W, Jang KK. Lithium–sulfur battery cable made from ultralight, flexible graphene/carbon nanotube/sulfur composite fibers. Advanced Functional Materials. 2016;**27**(4):1604815

[134] Biao Z, Feiyu K, Jean MT, Jang KK. Recent advances in electrospun carbon nanofibers and their application in electrochemical energy storage. Progress in Materials Science. 2016;**76**:319-380. DOI: 10.1016/j.pmatsci.2015.08.002

[135] Yong SK, Ghazal S, Yevgen Z, Jaehyuk L, Zhong L, Bharat P, et al. The critical contribution of unzipped graphene nanoribbons to scalable silicon–carbon fiber anodes in rechargeable Li-ion batteries. Nano Energy. 2015;**16**:446-457. DOI: 10.1016/j.nanoen.2015.07.017

[136] Xiaoyan W, Lian F, Decai G, Jian Z, Qingfeng Z, Bingan L. Core–Shell Ge@Graphene@TiO_2 nanofibers as a high-capacity and cycle-stable anode for lithium and sodium ion battery. Advanced Functional Materials. 2016;**26**(7):1104-1111. DOI: 10.1002/adfm.201504589

[137] Xiaoxin M, Guangmei H, Qing A, Lin Z, Pengchao S, Jinkui F, et al. A heart-coronary arteries structure of carbon nanofibers/graphene/silicon composite anode for high performance lithium ion batteries. Scientific Reports. 2017;**7**(1):9642. DOI: 10.1038/s41598-017-09658-4

[138] Jian Z, Guanhua Z, Xinzhi Y, Qinhong L, Bingan L, Zhi X. Graphene double protection strategy to improve the SnO_2 electrode performance anodes for lithium-ion batteries. Nano Energy. 2014;**3**:80-87. DOI: 10.1016/j.nanoen.2013.10.009

[139] Ji C, Chun L, Gaoquan S. Graphene materials for electrochemical capacitors. The Journal of Physical Chemistry Letters. 2013;**4**:1244-1253. DOI: 10.1021/jz400160k

[140] Liang H, Chun L, Gaoquan S. High-performance and flexible electrochemical capacitors based on graphene/polymer composite films. Journal of Materials Chemistry A. 2014;**2**:968-974. DOI: 10.1039/C3TA14511E

[141] Jing L, Xianke H, Linfan C, Nan C, Liangti Q. Preparation and supercapacitor performance of assembled graphene fiber and foam. Progress in Natural Science: Materials International. 2016;**3**:212-220. DOI: 10.1016/j.pnsc.2016.05.006

[142] Yue H, Huhu C, Fei Z, Nan C, Lan J, Zhihai F, et al. All-in-one graphene fiber supercapacitors. Nanoscale. 2014;**6**:6448-6451. DOI: 10.1039/C4NR01220H

[143] Yang Z, Qing H, Zhihua C, Lan J, Liangti Q. Integrated graphene systems by laser irradiation for advanced devices. Nano Today. 2017;**12**:14-30. DOI: 10.1016/j.nantod.2016.12.010

[144] Yunzhen C, Gaoyi H, Dongying F, Feifei L, Miaoyu L, Yanping L. Larger-scale fabrication of N-doped graphene-fiber mats used in high-performance

energy storage. Journal of Power Sources. 2014;**252**:113-121. DOI: 10.1016/j.jpowsour.2013.11.115

[145] Guan W, Pengfeng T, Xingjiang W, Lu P, Hengyang C, Cai FW, et al. High-performance wearable micro-supercapacitors based on microfluidic-directed nitrogen-doped graphene fiber electrodes. Advanced Functional Materials. 2017;**27**(36):1702493. DOI: 10.1002/adfm.201702493

[146] Yuning M, Yang Z, Chuangang H, Huhu C, Yue H, Zhipan Z, et al. All-graphene core-sheath microfibers for all-solid-state, stretchable fibriform supercapacitors and wearable electronic textiles. Advanced Materials. 2013;**25**(16):2326-2331. DOI: 10.1002/adma.201300132

[147] Bingjie W, Qingqing W, Hao S, Jing Z, Jing R, Yongfeng L, et al. An intercalated graphene/(molybdenum disulfide) hybrid fiber for capacitive energy storage. Journal of Materials Chemistry A. 2017;**5**(3):925-930. DOI: 10.1039/C6TA09360D

[148] Qiuyan Y, Zhen X, Bo F, Tieqi H, Shengying C, Hao C, et al. MXene/graphene hybrid fibers for high performance flexible supercapacitors. Journal of Materials Chemistry A. 2017;**5**(42):22113-22119. DOI: 10.1039/C7TA07999K

[149] Guoxing Q, Jianli C, Xiaodong L, Demao Y, Peining C, Xuli C, et al. A Fiber supercapacitor with high energy density based on hollow graphene/conducting polymer fiber electrode. Advanced Materials. 2016;**28**(19):3646-3652. DOI: 10.1002/adma.201600689

[150] Huhu C, Yaxin H, Gaoquan S, Lan J, Liangti Q. Graphene-based functional architectures: Sheets regulation and macrostructure construction toward actuators and power generators. Accounts of Chemical Research. 2017;**50**(7):1663-1671. DOI: 10.1021/acs.accounts.7b00131

[151] Luhua L, Jinghai L, Ying H, Yuewei Z, Wei C. Graphene-stabilized silver nanoparticle electrochemical electrode for actuator design. Advanced Materials. 2013;**25**(9):1270-1274. DOI: 10.1002/adma.201203655

[152] Jia L, Zhi W, Xuejun X, Huhu C, Yang Z, Liangti Q. A rationally-designed synergetic polypyrrole/graphene bilayer actuator. Journal of Materials Chemistry. 2012;**22**(9):4015-4020. DOI: 10.1039/C2JM15266E

[153] Zhibin Y, Hao S, Tao C, Longbin Q, Yongfeng L, Huisheng P. Photovoltaic wire derived from a graphene composite fiber achieving an 8.45% energy conversion efficiency. Angewandte Chemie International Edition. 2013;**52**(29):7545-7548. DOI: 10.1002/anie.201301776